CTI-CRYOGENICS

(7)

AD A093416

LEVEL II

DTIC
ELECTE
DEC 29 1980
C

DDC FILE COPY

HELIX
A Helix Company

DISTRIBUTION STATEMENT A
Approved for public release;
Distribution Unlimited

80 12 02 005

7

CLOSED CYCLE CRYOCOOLER FOR LOW TEMPERATURE ELECTRONIC CIRCUITS

PHASE I: CONCEPT STUDY

CONTRACT N00014-80-C-0465

F. William Pirtle, Program Manager

CTI-CRYOGENICS
A Division of Helix Technology Corporation
Kelvin Park
Waltham, MA 02154

12 75

Final Report
November 1980

Submitted to:

Office of Naval Research
Department of the Navy
800 N. Quincy Street
Arlington, Virginia 22217

TABLE OF CONTENTS

LIST OF FIGURES

LIST OF TABLES

FORWORD

This report is the final technical document describing the work accomplished under Office of Naval Research Contract NOC014-80-C-0465. The report describes the approach to and results of the Phase I study to develop concepts for closed cycle cryocoolers for low temperature electronic circuits.

Technical contributions to the program have been made by Ms. J.M. Kaufman and Dr. B. A. Andeen, of CTI-CRYOGENICS and by Dr. J. Nicol and Dr. M. Rona of Arthur D. Little, Inc.

Consultation and advice have been contributed by Mr. F. Chellis, and Dr. P.J. Kerney of CTI-CRYOGENICS.

NOMENCLATURE

Symbol	Definition	Units
A	Area	cm^2
a	Displacer radius	cm
C_G	Heat capacity of gas	j/K
C_p	Wall specific heat	j/gK
C_{PG}	Gas specific heat	j/gK
C_R	Heat capacity of regenerator	j/K
D	Displacer diameter	cm
E	Regenerator loss	watts
f	Operational frequency	cycles/sec
F	Form factor	
Hz	Frequency of operation	Hertz
H_{av}, h	Surface heat transfer coefficient	watts/cm^2K
H_o	Terrestrial field	guass
H	Magnetic field	guass
k	Thermal conductivity	watts/cmK
K_x	Shuttle loss constant	
k_g, cold	Thermal conductivity of cold gas	watts/cmK
K_g,k_o	Gas thermal conductivity	watts/cmK
k	Wall thermal conductivity	watts/cmK
L, x	Length	cm
L	Length of displacer	cm
m_g	Mass flow of gas	gram/sec
m	Logarithmic decrement	1/cm

NOMENCLATURE (Continued)

Symbol	Definition	Units
NTU_o	Number of Transfer Units	
P_L	Low pressure	atm
P_H	High pressure	atm
P_R	Pressure ratio	
P_{max}	Maximum cycle pressure	atm
P_{min}	Minimum cycle pressure	atm
P	Pressure	atm
ΔP	Pressure difference	atm
Pr	Prandtl number $\frac{C_{PG}\mu}{k_g}$	
Q_{gross}	Gross or Thermodynamic Cooling	watts
Q	Conduction Loss	watts
Q_{pump}	Pumping loss	watts
Q_{shut}	Shuttle loss	watts
Q_{RF}	Regenerative Friction loss	watts
Q_{reg}	Regenerator loss	watts
R	Gas constant	j/gK
S	Gap between displacer and cylinder	cm
ΔT	Temperature difference	K
T_a	Ambient Temperature (or temperature of next warmer stage)	K
T_e	Temperature of expansion chamber	K
T_{avg}	Average temperature	K
T	Temperature	K
V_{max}	Maximum Cold Chamber Volume	cm^3
V_{min}	Minimum Cold Chamber Volume	cm^3

NOMENCLATURE (Continued)

Symbol	Definition	Units
V	Volume	cm^3
V_{ar}	Impingement velocity	cm/sec
x	Thickness	cm
X_n	Slot characteristic dimension	cm
X	Magnetic susceptibility	
Z_o	Distance from mean position of end of displacer	cm
α	angle	radians
λ	Thermal penetration depth	cm
μ	Gas dynamic viscosity	g/cm sec
ρ	wall density	g/cm^3
ρ_o	Gas density	g/cm^3
θ	Temperature fluctuation amplitude	K
$\theta_{e,a}$	Temperature of gas next to wall	K
$\theta_{o,a}$	Temperature at surface of wall	K

I. ABSTRACT

The ultimate goal of the total program is to develop cryocoolers which operate at 4.2K with a heat load of at least 10 milliwatts. The goal of this Phase I effort is to conduct a conceptual study of small, low power, very low magnetic signature, lightweight, efficient closed cycle cryocoolers suitable for use with superconductive and other low temperature electronic circuits and systems. For this initial phase, the cryocoolers are to produce 50 milliwatts at 10K or less with electrical input power not to exceed 250 watts. Temperature fluctuations at the electronics of ± 0.01K or less are required. The cryocoolers are to have miniumum mechanical motion and magnetic signatures.

This study has examined various thermodynamic approaches and modeling. Regenerator geometries have been examined and regenerator materials have been screened, selected, and evaluated. Several configurations have been evaluated. Preliminary vibration and magnetic signature analyses have been performed on the most promising concepts.

Three primary concepts were selected. These are a small Macor concept, a large Macor concept and a Nylon concept. All have input power requirements between 140 and 210 watts. The small Macor concept is recommended for Phase II design and development because of its small size, ceramic construction and higher operating speed. An integral drive is recommended.

Conclusions are reached that the power goal is achievable as is the temperature fluctuation goal, but the vibration and magnetic signature goals require further definition and analysis. Other critical areas identified include helium permeation and ceramic residual iron.

Recommendation is made to proceed with a Phase II detailed design of the small Macor concept, and to proceed with approaches for solving the helium permeation, vibration and magnetic signature, and ceramic residual iron areas of concern.

II. INTRODUCTION

The United States Navy is currently developing cryocoolers to support superconducting electronics applications such as magnetometers and gradiometers. These applications have specific requirements and characteristics. The refrigeration requirement at the operating temperature of 10K is 50 milliwatts. However, a high degree of passive temperature control is required. Temperature variations of $\pm$ 0.01K or less are specified in order to obtain the thermal environment required by the electronics. State of the art magnetometers are sensitive to magnetic inputs on the order of 10^{-11} G $Hz^{-1/2}$ and gradiometers are sensitive to 10^{-12} $Gcm^{-1}Hz^{-1/2}$. Field instruments also exhibit about the same sensitivity. If these sensitivites are to be meaningful in practice, magnetic noise and mechanical motion inputs induced by the cryocooler within the effective bandwidth must be held to less than these values at the detector. Materials of construction should be limited to non-ferromagnetic materials because movement of magnetic materials through the Earth's magnetic field of 0.5 Gauss is sufficient to mask the attempted measurement. The use of any metal at all must be carefully considered because of the magnetic field problems. The study is to include a thermodynamic analysis of achieving the required refrigeration and temperature control as well as a study of the effect of the materials and method of construction on the critical magnetic requirements of the electronics.

Because of the critical nature of the magnetic signature criteria, CTI-CRYOGENICS has enlisted the consulting expertise of Arthur D. Little, Inc. Consultants from their staff have assisted as team members in the evaluation and assessment of magnetic signature and vibration associated with proposed concepts.

Purpose:

The purpose of this study is to propose closed cycle cryocooler concepts compatible with highly sensitive superconducting electronic systems.

Design Requirements

The cryocooler concepts are to achieve the following design specifications:

- An operating temperature of 10K or less for a heat load of 50 milliwatts is required.

- The ultimate operating temperature with no applied load is to be less than 8.5K.

- The temperature stability at the cold station for a heat load of 10 to 50 milliwatts is to be of the order of or less than $\pm$ 0.01K. This stability is to be achieved without the use of any electrical feedback system for temperature control.

- The ultimate goal of the program is the development of a cryocooler capable of achieving an operating temperature of 4.2K with a heat load of at least 10 milliwatts.

- The electrical input power should be minimized. The upper limit is 250 watts and a preferred value is 100 watts.

- Weight and volume are to be as small as possible consistent with the required thermal performance, minimum maintenance, and a long Mean Time Between Failures (MTBF).

- Magnetic signature and mechanical motion of the cryocooler at the cold station must be minimized. The goal of the magnetic signature and vibration criteria is to not interfere with measurements as small as 10^{-14} Tesla RMS (10^{-10} G RMS). This corresponds to a rotation in the earth's magnetic field of the order of 10^{-10} radians.

  Procedures are to be outlined for distinguishing between various possible mechanical motion and magnetic signatures and for identifying the sources of the signatures.

Scope:

The scope of the study includes the following:

- Concept or concepts are to be proposed which satisfy the design specifications.
- Provide back up material giving the basis for the performance and the method of selection.
- Provide back up material for the consultant's analysis of vibration and magnetic signature.

Summary:

In order to more closely satisfy the design specification for closed cycle cooling, Stirling refrigeration cycle concepts have been formulated. The Stirling cycle approach has been selected because it is the only mature thermodynamic cycle which offers the efficiency needed to meet input power requirements. The studies have included regenerators located in the cylinder wall using a solid displacer (the annular wall regenerator) and gap regenerators. Gap regenerators use the clearance between a solid displacer and the cylinder wall for the helium flow, and thermal penetration into the displacer piston and cylinder wall as the regeneration heat transfer.

Materials evaluated have included plastics, glasses, and metals. The plastics and glasses have more attractive magnetic properties. In addition they have low thermal diffusivity -- an advantage in gap regenerators.

Gap regenerators offer thermodynamic and magnetic field advantages, but also present other problems, e.g., helium permeation through the materials, and dielectric charge generation. Annular wall configurations have more difficulty in meeting the input power requirements because of the relatively large cross section area in the regenerator which leads to conduction losses. The small Macor concept using a gap regenerator has been selected as the most attractive candidate for further development and a plan for Phase II of that development is presented in this report. The small Macor concept offers

minimum size combined with a low input power requirement. Higher operating speed will provide a greater separation of cryocooler and electronics frequencies of operation. The shorter, lighter cold finger vibration amplitudes will be less than those of the larger concepts.

III. METHOD OF APPROACH, MODELING TECHNIQUE

Modeling of Stirling Cycle

In order to conform to the program schedule requirement, a CTI-CRYOGENICS proprietary mathematical model and the corresponding computer program was modified to provide thermodynamic performance predictions of the Stirling cycle for two specific geometries. These were the annular cylindrical wall regenerator and the gap regenerator geometries.

° Annular Wall Regenerator Geometry

The annular wall geometry, illustrated in Figure 1, has the advantage that the features of a metallic regenerator material, e.g. high specific heat, are available in a stationary regenerator matrix. A solid non metallic displacer can be used to move the gas through the regenerator. The non metallic displacer can be chosen to have minimum effect on magnetic signature. While vibration of the regenerator matrix and cylinder wall must still be minimized, the metallic regenerator matrix does not move as a consequence of carrying out the thermodynamic cycle.

The annular wall regenerator shown in Figure 1 is a six stage Stirling refrigerator. The displacers are solid so that helium gas cannot flow through them, but must flow through the annular regenerator areas located in the cylinder walls. The cylinder walls are in effect, hollow. The hollow space is filled with one or more materials that serve as heat storage volumes. These materials are generally porous so that helium can flow through and exchange heat with the material with a minimum of pressure drop. Helium enters the regenerator through several entrance passages shown as 45° ports at the top of each regenerator stage. The exit ports are shown as 45° ports at the bottom of each stage. When the displacer moves upward, the helium gas is displaced from the space above the displacer into the entrance ports. This represents the high pressure heat removal from the gas in the Stirling cycle. During the low pressure cooling of the regenerator, the displacer moves down and the entrance and exit port functions are reversed.

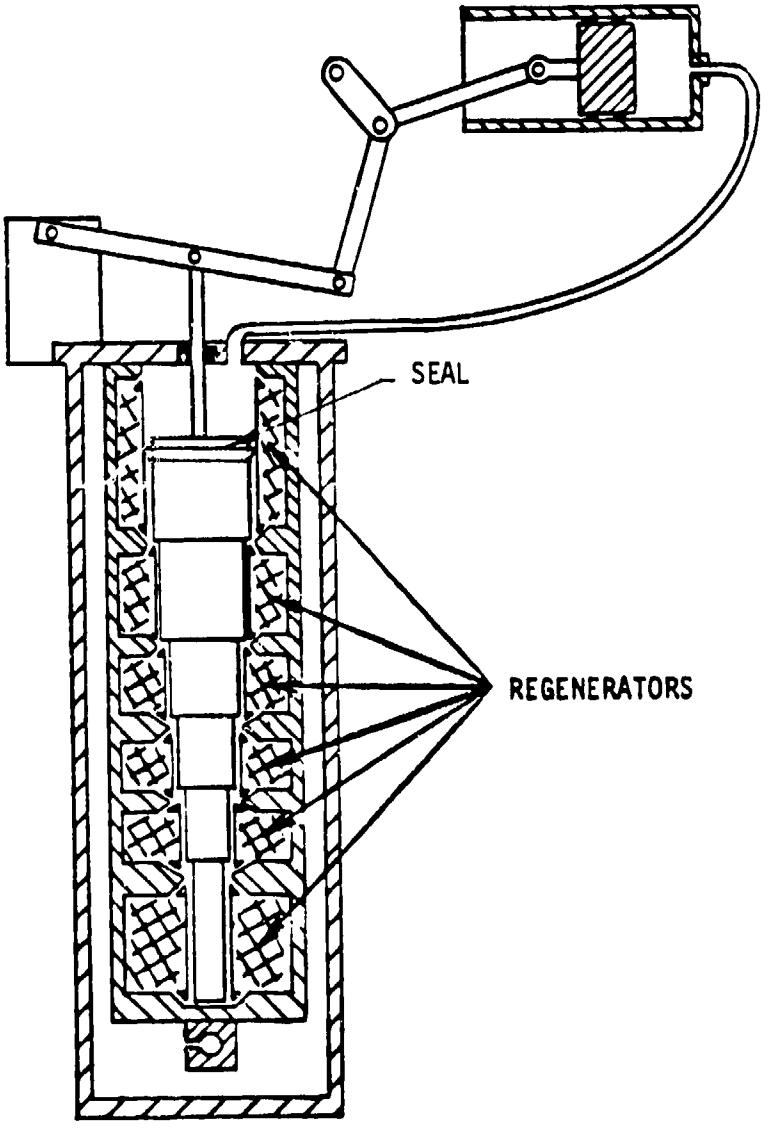

Figure 1: Annular Wall Regenerator Geometry

The inner wall of the cylinder may be a different material from the outer cylinder wall in order to reduce conduction heat losses. Since this inner wall has very little pressure drop, it can be made very thin. Its function is to divide the regenerator volume from the displacer volume. This wall is illustrated as a single line alongside the displacer in Figure 1.

There is a gap in Figure 1 between the displacer and the cylinder wall. This gap actually contains a seal to prevent gas from leaking around the displacer instead of traveling through the regenerator. The seal has been shown on the first stage only as an illustration.

° Gap Regenerator Geometry

The gap regenerator system is illustrated in Figure 2. Whereas other geometries such as the annular wall regenerator have specific volumes of regeneration material, the thermal regeneration in this geometry occurs by thermal penetration into the cylinder and displacer walls. When the displacer moves upward, helium flows downward in the gap between the cylinder and displacer. For displacer diameters on the order of 2 cm, the gap will be on the order of 0.01 cm. Heat transfer between the helium gas and the cylinder and displacer walls occurs by surface heat transfer. During the phases of the cycle, heat penetrates into and is removed from the walls in the fashion of a damped temperature wave propogating into a wall with periodically changing surface temperature. During the high pressure regenerative heat exchange, the displacer moves upward. The helium gas flows downward between the cylinder and displacer. Since the helium is warm from the compression that occurred previously, heat is transferred to the regenerator and the gas is cooled. The heat penetrates into the regenerator wall and is stored. After the expansion process to lower pressure, the displacer moves downward thereby displacing the cold helium upward through the gap. Heat is transferred to the helium thereby cooling the cylinder and displacer wall surfaces.

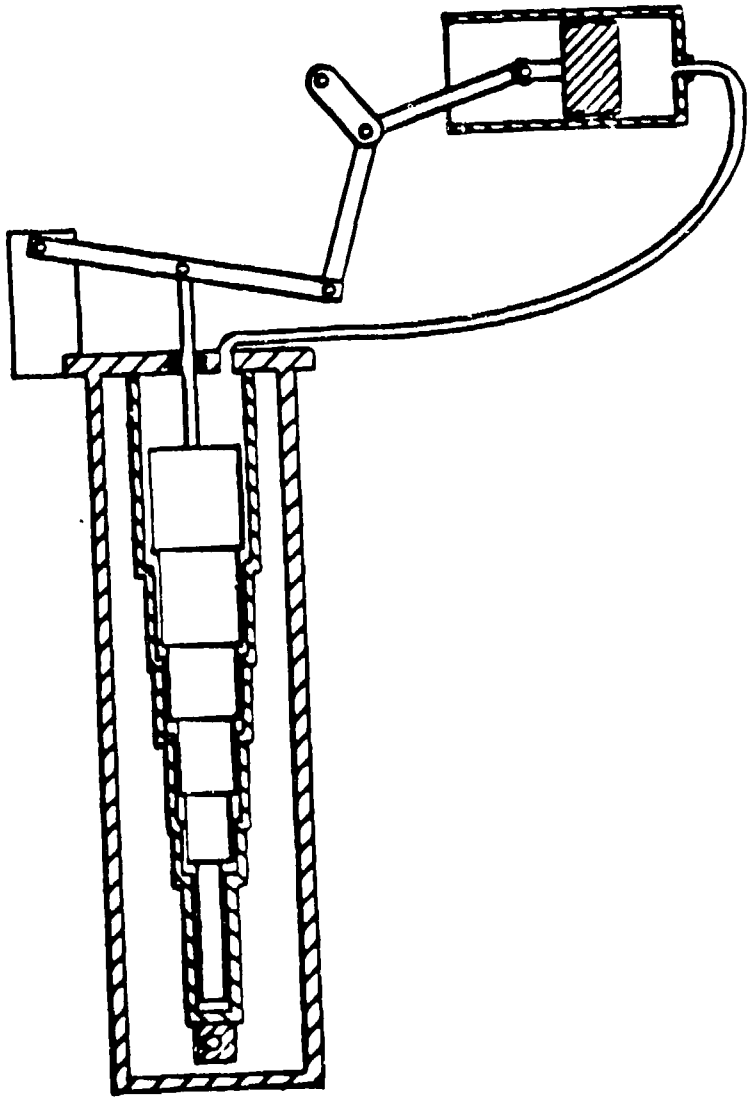

Figure 2: Gap Regeneratory Geometry

The rest of the hardware and process is represented by a standard Stirling refrigeration cycle. An integral compressor (compressor and cold finger connected by a common mechanical linkage) is illustrated, but any arrangement, e.g., the split system or gas driven system, used in Stirling cycles could be used in the gap regenerator geometry.

Modeling of Thermodynamic Performance [1]

The method of modeling the thermodynamic performance assumes that all the system losses can be decoupled from each other and calculated separately. The amount of useful cooling at the cold tip can then be calculated as the difference between the thermodynamic or gross cooling at the expander and all the losses acting on the gross cooling. The performance calculation then becomes a problem of identifying the gross cooling and the various losses. The principal losses are the conduction loss, shuttle loss, pumping loss, regenerator loss, regenerator friction loss, and seal frictional heat. The frictional seal loss doesn't occur in a gap regenerator geometry. The following discussion will identify the gross cooling and each of the respective losses.

Gross Cooling

Gross or thermodynamic cooling per cycle can be expressed as:

$$Q_{gross} = \oint PdV \qquad (1)$$

In the case of cycles where the PV cycle diagram is in large part rectangular and the cycle pressure changes are primarily determined by the pressures of source and sink lines, the thermodynamic cooling can be expressed as:

$$Q_{gross} = F\ (P_{MAX} - P_{MIN})\ (V_{MAX} - V_{MIN}) \qquad (2)$$

where F is a form factor between 0 and 1 to account for the lack of a completely rectangular cycle diagram. The Gifford-McMahon cycle is one example where the pressures of the source and sink represent the cycle maximum and minimum pressures very closely. In this case, a form factor may typically be on the order of 0.7.

In the case of a Stirling cycle, the PV diagram is typically more rounded. The value of F is therefore reduced. Also, the importance of knowing the correct F is increased. In order to determine the value of F to use if equation (2) is used for the gross cooling, the complete mathematical model was compared with experimental data on existing CTI-CRYOGENICS' Stirling cycle refrigerators. A resulting value of 0.6 for F provided agreement of the model with the data over the ranges of data available.

Conduction Loss:

The cold and warm ends of each stage of refrigeration are thermally connected by conductive paths through the displacer, cylinder wall, and regenerator (if present). These conduction losses can be calculated as

$$Q = \frac{k}{L} A \Delta T \qquad (3)$$

The thermal conductivity, k, is evaluated at the mean temperature of the section under consideration for displacer and cylinder wall conduction. For regenerator conduction, k is evaluated using the correlation found in Figure 11-7 of McAdams [2]. The correlation in McAdams is explicitly for spherical particles and stagnant interstitial gas. It doesn't address wire meshes and ignores packing pressure, which can affect the conductivity by changing the contact resistance between spheres. Nevertheless, the correlation is used to estimate the bed conductivity. The conductivity of wire mesh regenerators is estimated by assuming that they act as particulate regenerators with a void volume fraction of 0.5.

Shuttle Loss:

The shuttle loss is also called motional loss. It occurs because of a thermal gradient along the length of both the displacer and cylindrical cold finger. With the displacer at various positions relative to the cylinder, the thermal gradient is not the same in both of them. Therefore, there is a mismatch in local temperatures across the gap between the displacer and the cylinder. Heat transfer occurs across the gas in the gap in both directions depending on the relative positions of the

displacer and cylinder. The combination of displacer motion and gap heat transfer causes heat to be transferred from the warm to cold end of the stage which results in a loss. The form of the shuttle loss has been derived by Andeen [1] as:

$$Q_{SHUT} = \frac{K_s \, k_{g\,cold} \, DY^2 \, (T_A - T_e)}{SL} \qquad (4)$$

Pumping Loss:

The pumping loss occurs in annular wall and conventional regenerator geometries but not in the gap regenertor. It is a direct result of the clearance gap between the cold finger and the displacer. During pressurization, cold gas from the cold end is forced into this annular gap. Since this annular gap becomes warmer as the ambient end is approached, the cold gas becomes heated while traveling up the annulus. Likewise, upon depressurization, gas traveling back toward the cold end is cooled. However, due to the finite ineffectiveness of the annulus as a regenerator, the gas re-enters the cold end at a higher temperature than when it left. The net temperature gain results in an energy transport to the cold end (a heat leak). The formulation [1] used in the model is :

$$Q_{pump} = \frac{4}{3} \frac{L \, k_g \, S \, \Delta T}{\pi D} \left[\frac{\pi RPM \, Cpg \, DS \, \Delta P}{R \, T_{AVG} \, k_g} \right]^{1.6} \qquad (5)$$

Regenerative Friction Loss:

Gas flow through the regenerator will cause a pressure drop across the regenerator. Because of the pressure drop, the gas at the cold end undergoes a smaller cycle fluctuation than at the warm end. Therefore, Q_{gross} formulations such as equation (2) are overpredictive. The applied correction factor is a loss due to the pressure drop across the regenerator given by:

$$Q_{RF} = 2F \, \Delta P_{MAX} \, (V_{max} - V_{min}) \qquad (6)$$

Regenerator Loss:

The regenerator is functionally a heat exchanger because heat is cyclically exchanged between the helium gas and the regenerator matrix. As in any heat exchanger, there must be a temperature difference to act as a driving potential for heat transfer. If the temperature difference approaches zero, so does the local heat transfer. It follows that the regenerator cannot totally reduce the incoming gas temperature to the cold end temperature. This inability represents the largest single cycle loss in most regenerative refrigerator designs.

The formulation used in the mathematical model is based on the Kays and London [3] analysis. The regenerator loss can be expressed as:

$$Q_{REG} = (1 - \varepsilon)\, m_g\, C_{PG}\, (T_A - T_e) \qquad (7)$$

where $1-\varepsilon$ represents the ineffectiveness of the regenerator expressed as:

$$1-\varepsilon = 1 - \frac{NTU_o - \Omega}{1+NTU_o - \Omega} \qquad (8)$$

where:

$$\Omega = \frac{NTU_o}{C_R/C_g} - 1.66 \left[\frac{NTU_o}{C_R/C_G}\right]^{1/2} + \left[\frac{1}{C_R/C_G}\right]^{1/4}$$

Data Correlations:

Data correlations used in the mathematical model have been obtained from various sources. Specific heat data for solids has been taken from Corruccini and Gniewek [4] and other data from the TPRC Data Series [5]. Thermal conductivities from the TPRC Data Series [5] and from the WADD Technical Reports [6] have been used.

The correlations for the specific heat and compressibility factor for helium gas were obtained from Radebaugh [7]. The specific heat correlation is accurate to 2% for 0.5 atm to 25. atm and 10K to 300K. The compressibility factor correlation is also accurate to 2% for 1 atm to 5 atm and 6K to 300K. Since the lower limit of 10K on specific heat limits the range of

the correlation, some caution must be used in extrapolating the results to lower temperatures, e.g., to determine the 8.5K and 4.2K performance requested for this program.

Gap Model:

The mathematical model of the gap regenerator treats the walls of the cylinder and the displacer as infinitely thick. The periodic temperature changes of the helium gas produces a periodic change of the surface temperature of the cylinder and displacer walls. The change in surface temperature of the walls produces a temperature wave propagation into the walls. A treatment of this type of temperature distribution in an infinitely thick wall and the resulting heat storage during half a cycle can be found in Jakob [8]. A model of this type has been used by Radebaugh [9] in his analysis of regenerator inefficiency of Stirling cycle plastic displacers.

A temperature wave propagating into an infinitely thick wall decays in amplitude as an exponential function of the distance from the wall surface. The distance that is required for the temperature amplitude to decay to $\frac{1}{e}$ of its surface value can be found by:

$$\theta = \theta_{o,a} e^{-mx} \tag{9}$$

where m is the logarithmic decrement:

$$m = \sqrt{\frac{\rho C_p \pi f}{k}} \tag{10}$$

and is a function of the wall material properties and the speed of cyclic operation.

The fraction of the total infinite wall heat storage that is stored in a finite wall thickness can be related to the number of decrements represented by the thickness, λ. By specifying the wall thickness as a multiple of decrements, the cylinder wall thickness required can be determined. The annular thickness on the outside of the displacer that acts as a regenerator was similary treated.

As the temperature is decreased, as in the colder stages of refrigeration, material k and Cp values change so the logarithmic decrement also changes. The wall thickness that is required increases with decreasing temperature. The concept cold stage wall thicknesses are therefore larger.

Thermal Damping:

Thermal damping is required to reduce the temperature fluctuations of the helium gas in the cold end to the $\pm$ 0.01K required at the electronics. The damping or effective temperature control must be passive. No electronic feedback systems can be included.

The treatment of damping is based on damped temperature waves similar to those occurring in the gap regenerator and reference is made to section 14-3 of Jakob [8].

Consider that the helium gas in the coldest stage has a temperature fluctuation half amplitude of $\theta = \theta_{e,a}$. The surface of the inside end of the cold finger in contact with the helium has a temperature amplitude of

$$\theta_{o,a} = \theta_{e,a}\,\eta \tag{11}$$

where:

$$\eta = \sqrt{\frac{1}{1 + \frac{2m}{b} + \frac{2m^2}{b^2}}} \tag{12}$$

where:

m = logarithmic decrement for the damping block

$$m = \sqrt{\frac{\rho C_p \pi f}{k}}$$

and b is defined as:

$$b = \frac{h}{k_w} \tag{13}$$

The surface heat transfer coefficient, h, was evaluated using the General Electric correlation [10] for an impinging jet flow from a slot nozzle:

$$\frac{h_{av}x_n}{k_o} = 0.36 \left[\frac{\rho_o V_{ar} x_n}{\mu_o}\right]^{.62} Pr^{.333} \qquad (14)$$

The velocity, V_{ar}, was evaluated by assuming that the helium gas flowed into the expansion chamber during 1/4 of the cycle time.

The temperature amplitude distribution inside the thermal damping block is given by Jakob as a function of the distance, x, from the cold surface as:

$$\theta = \theta_{o,a} e^{-mx} \qquad (9)$$

Combining equations (9) and (11) yields:

$$\theta = \theta_{e,a} ne^{-mx} \qquad (15)$$

Using the properties of the helium gas, the refrigeration cycle pressures, speed, and the properties of the damping material selected, the temperature fluctuation amplitude can be found as a function of the length of the damping block.

The other consideration is that the temperature drop from the electronics to the cold gas must be as small as possible so that the cold gas temperature drop below 10K can be held to a minimum. The total temperature potential necessary to transfer the required amount of heat is:

$$\Delta T = \frac{q}{hA} + \frac{q\,x}{kA} \qquad (16)$$

The temperature fluctuation of equation (15) must be held to a minimum . The temperature drop of equation (16) must also be minimized. These criteria suggest the selection of a material for the damping block that has a high thermal conductivity and a low thermal diffusivity. In other words, while the thermal conductivity must be high enough for an acceptable ΔT, the volumetric heat capacity must be high relative to the thermal conductivity in order to obtain the heat capacity necessary for damping. Given

these criteria, a material such as lead becomes attractive for thermal damping. The length of the damping block can be adjusted to fit the cryocooler concept geometry and speed to provide effective damping.

Lead is diamagnetic with a magnetic susceptibility of about 1/4 that for helium gas. Therefore, the effect of the lead block on magnetic signature will be minimal above the superconducting transition temperature of 7.2K. Below this temperature, lead is superconducting and will exclude magnetic fields.

The model for thermodynamic performance including the model of the gap geometry combined with the data correlations is sufficient to determine the thermodynamic performance of candidate cryocoolers. When this is combined with the model for thermal damping, the performance of candidate cryocoolers can be compared with the program thermodynamic specifications. These models were used to determine the performance of the concepts that are presented in the following sections.

IV. CONCEPT DESCRIPTION

Drive System Concepts

The cryocooler concepts have three subsystems. These are the drive system, cold finger, and thermal damping system. The method of modeling the cold finger and thermal damping systems has been previously discussed. A brief discussion of methods of driving the cold finger and their relative advantages and disadvantages follows.

The cryocooler drive system can either be an integral drive (Stirling compressor and cold finger drive are connected by a common kinematic linkage to the drive motor) or a split system (gas or hydraulic drive operates the cold finger). The motor and compressor can be separated from the cold finger in the split cycle arrangement. The split system advantages over an integral system are lower motor caused magnetic fields and more packaging flexibility. The disadvantages are greater difficulty in balancing the displacer (more vibration), possible short stroking (short stroking occurs when the displacer moves less than the design stroke), and higher power requirements. Short stroking of the displacer can occur at low temperatures so that the gross cooling is reduced. Changes in pressure drop across the displacer at low temperatures produce a change in seal friction which can cause the displacer to move less than the design stroke. The result is a decrease in thermodynamic performance. The power requirement is somewhat higher because of line losses associated with the separation length of the transfer line and because the split cycle compressor and cold finger phase angle can vary from the optimum. The power increase because of these effects depends on the length of the transfer line from the compressor to the cold finger.

The primary concepts will be shown with an integral drive because it can be more closely balanced thereby giving less vibration and it will require less input power because the line loss is less. The integral concept will also have more consistent thermodynamic performance. Mu metal shielding of the motor is required to attenuate the motor caused magnetic field. This problem is more acute with an integral system because of the proximity of the motor to the cold end. Shielding is required with either an integral or split system to attenuate the motor magnetic fields, however.

Annular Wall Concept

Several concept variations were performed on an annular wall concept with the object of reducing the power input to within the program goals. Specifications of the best concept resulting from the investigation are given in Table 1.

The required thermodynamic power was determined from the mathematical model. This thermodynamic power was increased to cover mechanical losses based on past experience. A 50% electric motor efficiency was then applied. The corresponding electrical input power is approximately 1200 watts. Therefore this concept exceeds the input power requirements of the program. The problems occur in conduction losses because of the stainless steel walls, and the regenerator wire mesh and lead balls. Plastic or glass walls will reduce these losses somewhat. The choice of an alternative regenerator bed material is more difficult. Because of the low thermodynamic performance of the concept compared to the gap regenerator, the investigation was discontinued.

Gap Concepts

Nine configurations formulated using the gap regenerator geometry are reported. Thermodynamic results are presented in Table 2. Three of the configurations have been used as the basis for concept drawings and are considered to be the most attractive candidates for further development. These are the Large Macor (number 8), Nylon (number 7) and the small Macor (number 9) configurations. Preliminary versions of the three primary configurations were provided to Arthur D. Little, Inc. for their vibration and magnetic signature analysis. The report of that analysis follows the description of the three concepts.

Table 3 is a gap configuration trade off table that summarizes the advantages and disadvantages of the gap configurations. The purpose of Table 3 is to summarize the numerical results of Table 2 and to present a qualitative discussion to indicate the advantages of the best configurations.

TABLE 1

ANNULAR WALL CONCEPT RESULTS

Number of Stages	4
Speed, RPM	225
Input Power, Watts	1200
Stage Temperature, K	150/87/30/10
Stage Capacity, Watts	0.579/0.354/0.166/0.050
Cylinder	
° Material	Stainless Steel
° Outer Wall Thickness, cm	0.04/0.04/0.04/0.04
° Inner Wall Thickness, cm	0.04/0.04/0.04/0.04
Regenerator	
° Material	Wire mesh/Wire mesh/Wire mesh/Lead balls
° O.D., cm	7.19/4.33/3.12/1.37
° I.D., cm	5.16/3.25/2.36/0.71
° Annular Thickness, cm	1.02/0.54/0.38/0.33
Displacer	
° Material	Nylon
° Diameter, cm	5.08/3.18/2.29/0.64
Stage Length, cm	10.2/9.5/9.5/8.9
High Pressure, atm	10.2
Low Pressure, atm	6.5
Stroke, cm	1.02

*Stage figures given are from warm end to cold end.

Table 2

Gap Configuration Thermodynamic Results

	(1)	(2)	(3)
Displacer/Cylinder Material	Nylon/St.Steel	Quartz/Quartz	Nylon/Macor
Number of Stages	4	4	4
Speed, RPM	60	85	120
Input Power, Watts	479	161	177
Stage Temperature, K	180/80/30/10	180/80/30/10	180/80/30/10
Stage Capacity*, Watts	0.120/0.026/0.150/0.050	0.298/0.035/0.245/0.050	0.187/0.152/0.013/0.05
Stage Diameters*, CM	4.13/2.86/1.98/1.21	2.70/1.91/0.142/0.79	1.91/1.59/1.27/i.02
Stage Length*, CM	38.1/28.1/20.5/25.4	10.2/10.2/10.2/15.2	10.2/10.2/7.6/15.2
High Pressure, atm	7.8	7.1	7.1
Low Pressure, atm	2.8	2.8	2.8
Wall Thickness*, CM	0.16/0.16/0.25/0.40	0.16/0.16/0.25/0.40	0.16/0.16/0.25/0.40
Stroke, CM	0.70	0.95	0.70

*Stage figures given are from warm end to cold end.

Table 2 (Cont.)

Gap Configuration Thermodynamic Results

	(4)	(5)	(6)
Displacer/Cylinder Material	Macor/Macor	Macor/Macor	Nylon/Nylon
Number of Stages	2	3	4
Speed, RPM	95	95	2000
Input Power, Watts	291	209	182
Stage Temperature, K	50/10	140/50/10	180/80/30/10
Stage Capacity*, Watts	0.317/0.050	0.386/0.088/0.050	0.156/0.277/0.138/0.050
Stage Diameters*, CM	2.82/1.02	3.02/1.57/1.02	0.89/0.76/0.53/0.28
Stage Length*, CM	25.4/15.2	12.7/12.7/15.2	5.1/5.1/5.1/5.1
High Pressure, atm	7.1	7.1	7.1
Low Pressure, atm	2.8	2.8	2.8
Wall Thickness*, CM	0.16/0.40	0.16/0.25/0.40	0.08/0.08/0.08/0.08
Stroke, CM	0.95	0.95	0.25

*Stage figures given are from warm end to cold end.

Table 2 (Cont.)

Gap Configuration Thermodynamic Results

	(7)	(8)	(9)
Displacer/Cylinder Material	Nylon/Nylon	Macor/Macor	Macor/Macor
Number of Stages	4	4	4
Speed, RPM	60	107	2000
Input Power, Watts	142	217	166
Stage Temperature, K	180/80/30/10	180/80/30/10	180/80/30/10
Stage Capacity*, Watts	0.277/0.062/0.111/0.050	0.316/0.072/0.045/0.050	0.164/0.138/0.123/0.1
Stage Diameters*, CM	2.5/1.91/1.65/1.11	2.38/1.91/1.27/1.02	0.89/0.76/0.53/0.28
Stage Length*, CM	15.2/15.2/10.2/15.2	10.2/10.2/10.2/15.2	5.1/5.1/5.1/2.5
High Pressure, atm	7.1	7.1	7.1
Low Pressure, atm	2.8	2.8	2.8
Wall Thickness*, CM	0.16/0.16/0.25/0.40	0.16/0.16/0.25/0.40	0.08/0.08/0.08/0.13
Stroke, CM	0.70	0.95	0.25

*Stage figures given are from warm end to cold end.

TABLE 3

GAP CONFIGURATION TRADE OFF TABLE

CONFIG-URATION	DISPLACER/CYLINDER MATERIAL	NUMBER OF STAGES	SPEED RPM	INPUT POWER WATTS	TOTAL LENGTH OF STAGES, CM	RELATIVE RIGIDITY	RELATIVE HELIUM PERMEATION	RELATIVE VIBRATION MOVEMENT	MAGNETIC SIGNATURE	REMARKS
1	Nylon/St. Steel	4	60	479	112	Very high	Very low	Very low - because of high rigidity	High iron content of stls. stl. will be a problem.	Power requirement larger than upper limit.
2	Quartz/Quartz	4	85	161	46	Moderate	Moderate	Moderate	Some residual iron.	Helium permeation higher than Macor
3	Nylon/Macor	4	120	177	43	High	Low	Low	Residual iron can be reduced.	Should avoid different materials because of thermal expansion problems.
4	Macor/Macor	2	95	291	41	High	Low	Low	Residual iron can be reduced	Power requirement larger than upper limit.
5	Macor/Macor	3	95	209	41	High	Low	Low	Residual iron can be reduced	Power requirement is higher than small 4 stage.
6	Nylon/Nylon	4	2000	182	20	Low	High	Low rigidity will result in larger movement	Can have very low susceptibility	Low rigidity is a problem as is high helium permeation.
7	Nylon/Nylon	4	60	142	56	Low	High	Low rigidity will result in larger movement	Can have very low susceptibility	Low ridigity more of a problem than in small Nylon.
8	Macor/Macor	4	107	217	46	High	Low	Low	Residual iron can be reduced	Not fully optimized. Power requirement will be lower than 3 stage.
9	Macor/Macor	4	2000	166	18	High	Low	Low	Residual iron can be reduced	Combines low power, high rigidity, low helium permeability and small size.

The 2 stage Macor and Nylon/Stainless Steel configurations have input power requirements which exceed the 250 watt limit. All of the other configurations in Tables 2 and 3 generally have power requirements of 150 to 200 watts. This includes the increase of thermodynamic power to cover mechanical and compressor efficiencies per past experience, and the electric motor efficiency using a Western Gear Co. P/N 504720 motor as a typical drive motor for determining power requirements.

The first configuration reported in Table 2 is comprised of a stainless steel cylinder and Nylon displacer. Stainless steel has the advantage that it is essentially impervious to helium diffusion flow through it. Even though the iron content of stainless steel is an indication of magnetic signature difficulties, a gap configuration was developed thermodynamically using stainless steel as a basis of comparison. A Nylon displacer was used to keep the conduction losses to a minimum. The results of the thermodynamic analysis listed in Table 2 show that the input power requirement is above the upper limit allowed in the program. The high thermal conductivity of the cylinder contributed to the higher conduction loss particularly in the warmer stages where the conductivity of stainless steel is high. To overcome the loss, a higher helium mass flow is required and this leads to the high power requirement. Therefore stainless steel is not attractive because of high input power as well as the magnetic problems because of the iron content.

Ceramic materials have been investigated. A quartz configuration is reported as the second configuration in Table 2. The cylinder and displacer are both of quartz construction. Input power is within the program limit. The helium permeability is relatively high, however, and it also contains residual iron. An aluminum oxide ceramic, Coors AD995, was also investigated. The thermal diffusivity is 450 times higher than Macor (the primary configuration material) at 10K. A high thermal diffusivity means a poorer thermodynamic material for gap regeneration. The thermal conductivity is greater than that of stainless steel at 10K. This is a factor of about 17 greater than that of Macor. The specific heat is about 40 times lower than Macor at 10K. The high thermal conductivity translates to higher conduction loss in the walls. Low specific heat leads to a thicker wall requirement for regeneration. The aluminum oxide was therefore judged inferior to Macor.

After extensive material search and analyses, Macor appears to be the optimum material for this application because of low thermal conductivity, low thermal diffusivity, good rigidity, and low magnetic susceptibility. The Macor is Code 9658 Machineable Glass Ceramic (MGC) produced by Corning Glass Company. Its helium permeability is at least two orders of magnitude less than Fused Silica (quartz). The first Macor configuration is constructed of a Macor wall and a nylon displacer. The thermodynamic results are shown in the third column of Table 2. It is thermodynamically competitive with regards to power requirement and size. One of the problems with construction of different materials is thermal contraction. The change in dimensions from room temperature to cryogenic temperatures can produce gaps that are too large or length changes leading to a large expansion chamber clearance volume. These effects are discussed in the literature [11]. Because of differential contraction problems, an effort was made to use the same material for both the cylinder and the displacer.

An investigation was conducted to determine the number of stages required in a gap configuration of Macor construction. The results of thermodynamic studies of 2, 3, 4 stage Macor configurations are listed in columns 4, 5 and 7 of Table 2. The 4 stage configuration shown is not fully optimized, but it should require less power so it was chosen as a primary configuration and will be discussed as the Macor concept later.

A small nylon configuration with a nylon cylinder and displacer was formulated and is reported in column 6 of Table 2. It is competitive with regard to power and size. However, the elastic modulus of nylon is low enough that the dimensional changes that may occur because of the cyclic internal pressure changes can likely be a source of vibration for the electronics package. A more rigid material is to be preferred if it is acceptable with regard to the other criteria.

The Macor and nylon configurations listed in columns 7, 8, 9 of Table 2 are the primary configurations. Four stages were used because of the results of studying 2, 3, 4 stages of Macor construction. Although the 3 stage configuration requires slightly less power, a full optimization will show that there is a lower input power requirement for four stage systems. Five stage systems would require even less power, but with diminishing returns. The power

requirement decrease is marginal and the additional stage adds complexity to the system. Four stages result from a trade off between input power and complexity.

The thermal damping study indicates that lead blocks of the sizes shown in the primary configurations will reduce the temperature fluctuations down to the required $\pm$ 0.01K. Lead is the only feasible material identified for damping at this time. Material feasibility is based on a high thermal conductivity to minimize the required temperature difference to transfer the heat at 10K, a very high specific heat to serve as a thermal capacitor, and reasonable ease of fabrication. Helium also possesses a high specific heat but the gas would have to be contained in a solid material. The gas interaction with the container requires two surface heat transfers resulting in additional temperature drops to transfer the heat. No ceramic material with satisfactory damping properties was found. The lead is diamagnetic above the superconducting transition temperature of 7.2K. Below the superconducting transition temperature, the Meissner effect of magnetic field exclusion will cause gross distortions of the magnetic field adjacent to the electronics package. In this case, an alternate means of thermal damping would be needed. However, lead is satisfactory at the 8.5K and 10K temperatures that are primary in the present program.

Drive motors are 400 Hz geared motors. AC motors are recommended instead of DC motors in order to achieve the minimum magnetic signature. Mu metal shielding of the motor is a requirement to attenuate the magnetic field. The motor used to determine the input power of the concepts studied is manufactured by Western Gear Company (model number P/N 504720). This motor was selected as a nominal representation of 400 Hz geared motors and was utilized to quantify the input power for each gap configuration.

In order to achieve the 10^{-10} radians or less of electronics rotation, a 10 inch long cold finger (approximately the length of the small Macor configuration) can only have a vibration amplitude of 10^{-9} inches. Even with a mechanically soft mount and internal damping, the only way to achieve this low vibration amplitude may be by electronics isolation and/or electronic suppression of the vibration noise. Still, the natural frequencies of the primary concepts are at least a factor of 7 higher than the operating frequency. This will help limit the effect of vibration. The small Macor

concept operating speed of 2000 RPM provides a sizeable buffer between it and the operational frequencies of magnetometers. The well defined frequencies will allow an electronic suppression system to be defined with reasonable results expected. The electronic suppression is probably best handled in an integrated system design including the cryocooler, electronics, and aircraft system or ground based installation.

Nylon Concept

The Nylon configuration was selected for a primary concept because it has a very small magnetic susceptibility, has a very low thermal conductivity at low temperatures, and can be fabricated readily.

The nylon concept is shown in Figure 3. It has four stages. Cold finger length is 56.5 cm. Thermal damping requires a lead block with a diameter of 1.42 cm and 4.73 cm long mounted on the end of the cold finger. An estimated space of 1.42 cm diameter and 2.54 cm long is provided for the electronics. Inclusion of radiation shields at the 180K and 80K stages and the vacuum shell makes an overall cold section length of 65.4 cm. The overall diameter of the vacuum shell is 5.0 cm.

The gap thicknesses for the four stages are 0.05 cm, 0.04 cm, 0.02 cm, and 0.01 cm. The gaps are not shown in Figure 3 because of their small size.

Operating speed is 60 cycles/min making this the slowest speed configuration. The stroke is 0.70 cm.

The compressor will need to be designed in detail. The bore is 4.01 cm and the compressor stroke is 0.70 cm. The features of the compressor design will be described in the Small Macor discussion.

The thermodynamic input power requirement is 50.2 watts. Using the efficiency of the P/N 504720 motor, electrical input power is 142 watts. This configuration has the lowest power requirement of any configuration formulated in this study.

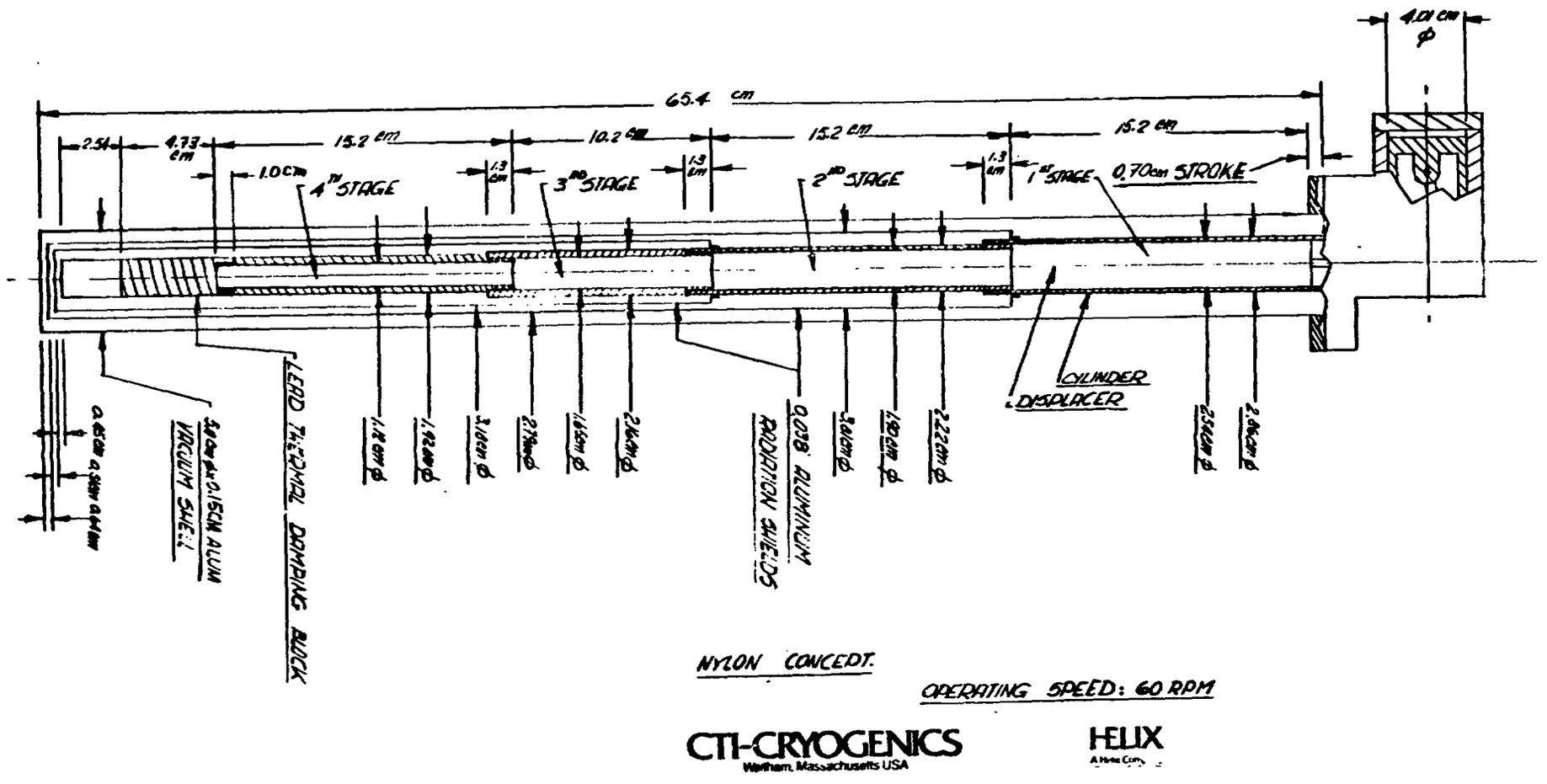

Figure 3: Nylon Concept

Macor Concept

The larger slower speed Macor configuration was used for the concept shown in Figure 4. Operating speed is 102 RPM and the stroke is 0.95 cm. Cold finger length is 77.0 cm. The damping block is 3.86 cm long, has a 1.82 cm diameter and is constructed of lead. When this block, estimated space for the electronics, radiation shields, and the vacuum shell are added, the total cold finger length is 84.8 cm. The diameter over the vacuum shell is 4.75 cm.

The gaps forming the regenerator from the warm to the cold stage have thicknesses of 0.025 cm, 0.020 cm, 0.020 cm, 0.010 cm. These thicknesses resulted in approximately optimum regeneration performance.

The compressor construction is aluminum. The stroke is 0.95 cm and the bore is 8.0 cm. The compressor internal details are not shown in Figure 4, but the same features are incorporated as are described in the small Macor concept (Figure 5).

Magnetic signature figures are given in the Vibration and Magnetic Signature Section. Since the configuration has the longest cold finger length, the motor is furthest from the electronics. Therefore, this configuration will have the lowest motor noise at the electronics. Since motor noise can be attenuated with shielding, this may not be of great advantage. The lower operating speed may be a disadvantage since its signature may be closer to the range of electronics frequencies of interest.

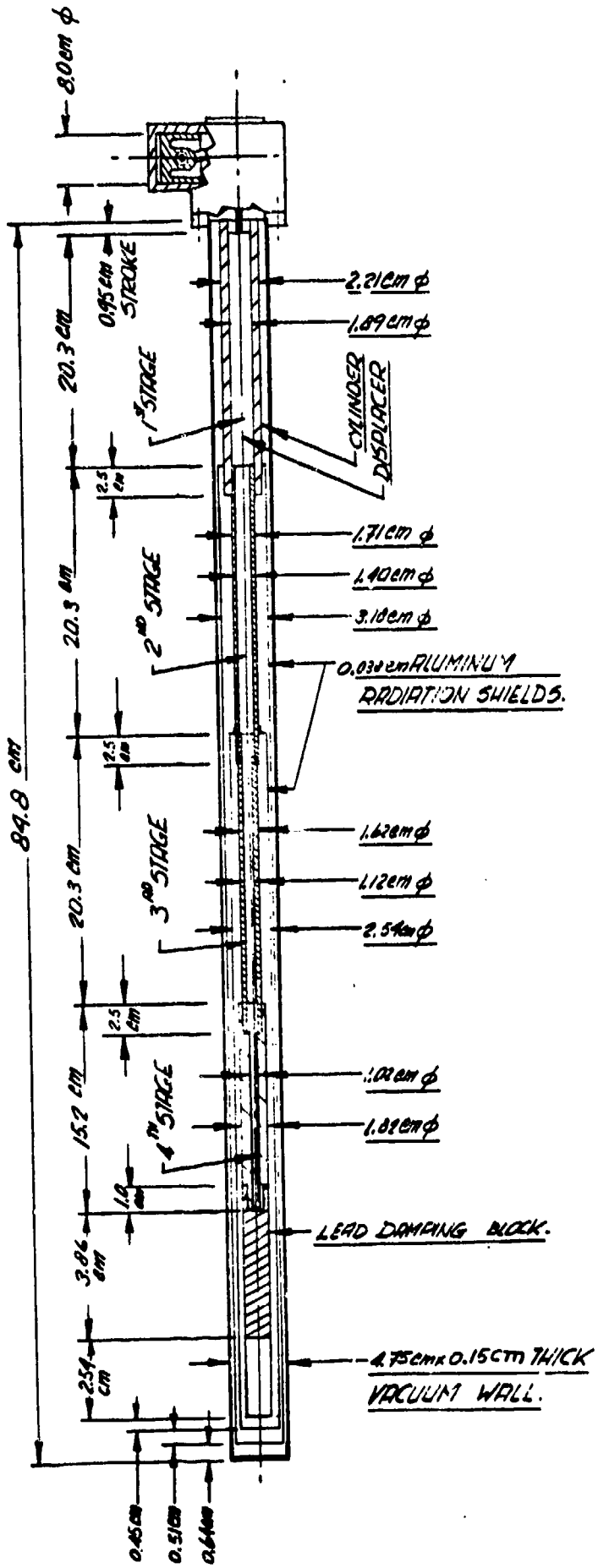

Figure 4: Macor Concept

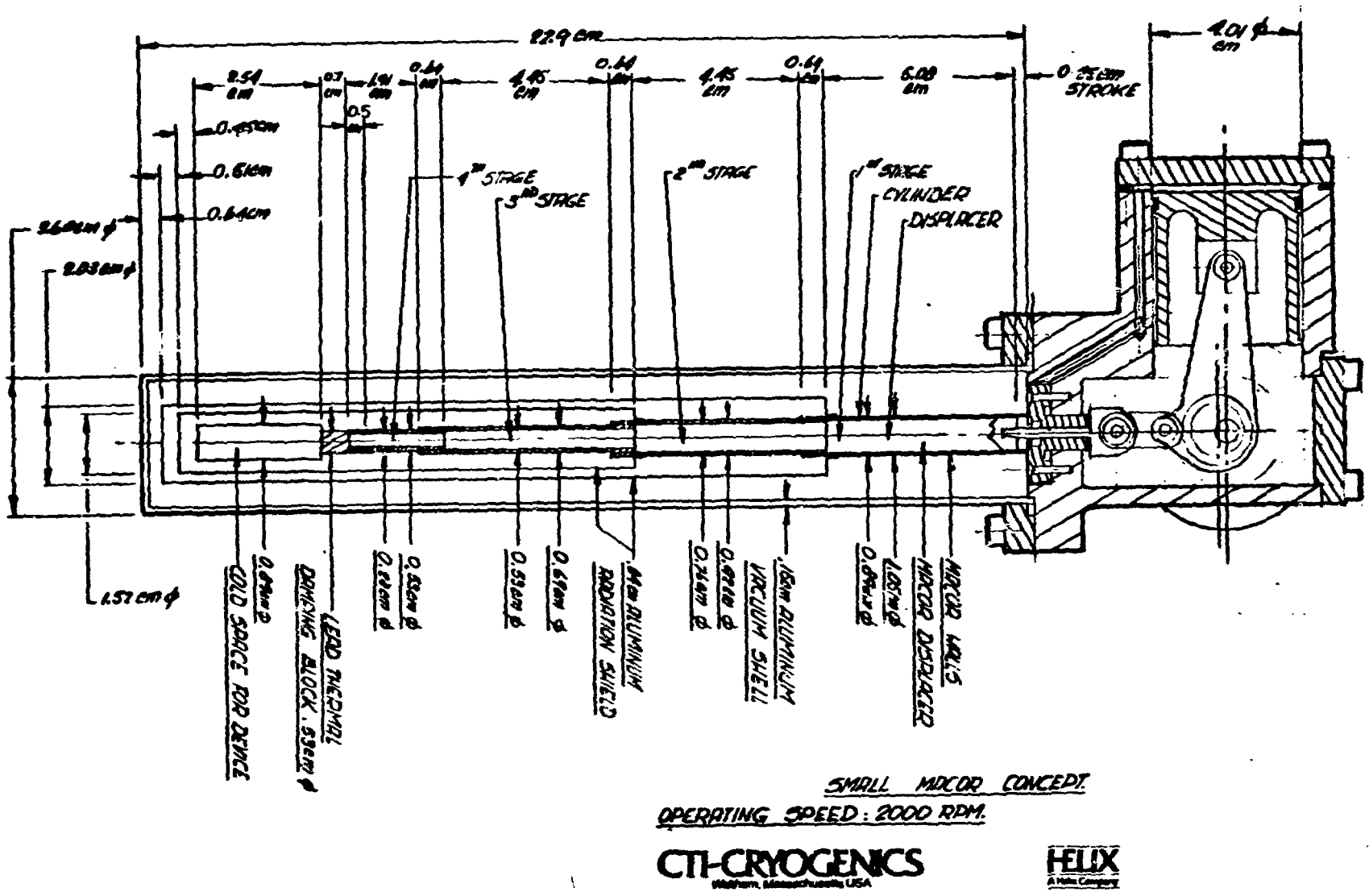

Figure 5: Small Macor Concept

Small Macor Concept

The small Macor concept is shown in Figure 5. A summation of the stage lengths from Table 2 gives an overall length of the cold finger of 18.1 cm. When the damping block, estimated space for the electronics, radiation shields, and vacuum shell are added, the length is 22.9 cm. The diameter over the vacuum shell is 3.68 cm. The concept has four stages as shown in the drawing. Wall thicknesses change somewhat with stage as shown in Figure 5. The cylinder wall thickness for each stage is a compromise between sufficient wall thickness to use the infinite wall model while minimizing the axial thermal conduction loss.

The cylinder wall is shown as the thin cross hatched section with the solid displacers located inside. The gaps that act as the regenerators are too small to show on the drawings. The gap thicknesses are 0.01 cm for all four stages.

The stroke of the cold finger is 0.25 cm. The stroke is the result of a trade off between minimizing the shuttle loss with small stroke, achieving refrigeration power, and reasonable operating speed and size.

The lead thermal damping block diameter is the same as the coldest stage diameter. The required length to damp the cold gas temperature oscillation inside the cold stage to the required 0.01K is 0.7 cm. A fluctuation of the temperature of the cold gas in the cold finger of 2K was used in analysis. Preliminary calculations indicate that this is about the maximum for the pressure ratios used in this study.

The compressor is shown in Figure 5. The bore is 4.0 cm and the stroke is 0.25 cm. Construction of aluminum is proposed. The arrangement shown in the drawing provides that any helium that leaks past the lip seal on the compressor or the stem packing on the cold finger is contained in the crank chamber. In initial charging, the crank chamber is charged with helium to the mean operating pressure. The lip seal will preferentially leak from the crank chamber to the compression chamber. Any small helium leaks during the high pressure phases of the cycle are replaced by crank chamber helium during the low pressure phases of the cycle. Therefore, there is no path for helium to leak out of the system.

Magnetic field, motion and vibration induced magnetic signature are summarized in the Vibration and Magnetic Signature Section. Sources of magnetic signature are discussed in the Magnetic Signature Section. Since this configuration is smallest, the electric motor (in an integral arrangement) is closest to the electronics. Therefore, the motor caused field is larger. Also, the length of the damping block that is required is less because of the higher frequency of operation. It would be of advantage, as far as displacer field distortion is concerned, to put a copper rod on the end of the damping block to extend the electronics away from the cold finger. At the same time, the copper extension would lengthen the cantilever cold finger and thereby lessen the vibration frequency and increase the amplitude. Both are adverse effects. While the various signatures have been identified and some of them quantified, the trade offs of placing the electronics on an extended bar are difficult to quantify in a concept study. A technique of isolating the electronics from the cold finger and using a flexible copper strap to conduct the heat from the electronics to the refrigerator is a possibility. In this case, the entire arrangement needs to be inside the radiation shields and vacuum shell.

The operating speed of the small Macor configuration was selected at 2000 RPM. The 2000 RPM was judged appropriate as an upper limit of speed from past experience with the trade off between size, life, and reliability. With further development, smaller sizes at higher speeds may prove to be even more attractive. The small Macor concept therefore, has the highest beam vibration frequency. Other factors being equal, this is preferred because the vibration noise will be far from the signal band of interest. It may be possible to make a smaller cold finger that operates at even higher frequencies. The trade off is the smaller size at higher speed compared with reliability or Mean Time Between Failures.

There are critical areas to be addressed when using Macor as a cold finger material. Macor is permeable to helium. Static electricity is generated in moving non conductors. Approaches to solving these problems have been identified and are discussed in the critical areas section.

Residual iron in the Macor ceramic will need to be minimized to produce an acceptably low magnetic susceptibility. This ceramic has very attractive thermal properties--low thermal conductivity and high specific heat. It does have the problem associated with many ceramics in that residual iron from the raw materials, specifically magnesium oxide, is present in normal amounts of about 500 parts per million. Efforts have been exerted at Corning to reduce the residual iron to an absolute minimum.

Configurations 4, 5 and 8 are Macor with 2, 3, and 4 stages respectively. Table 2 indicates that the three stage configuration requires less power than either the two or four stage configurations. This is because the configurations are not fully optimized. The three stage configuration requires about the same power as the four stage. If the configurations were fully optimized, the trend would be decreasing power requirement with increasing number of stages, but with diminishing returns. The four stage concept does not have as much of an advantage over the three stage configuration as the three stage configuration has over the two stage. Similarly a five stage system would have even a smaller power advantage over the four stage system. At some point, the increase in complexity is not justified by the decrease in input power obtained by additional stages. The graph of this trend is included in the thermodynamic performance section. From the discussion in that section, four stages appears to be a reasonable trade off between input power and complexity.

Nylon appears attractive thermodynamically because its low thermal conductivity produces low conduction losses and reasonable regenerator depths in the gap system. A nylon configuration was included as a primary configuration (number 7) because it is thermodynamically a promising material. The high speed nylon configuration (number 6) requires somewhat more power. The low rigidity of nylon will likely cause more vibration at the electronics caused by nylon cyclical stretching during the pressure cycling of the refrigerator. The elastic modulus of nylon is more than 10 times less than that of Macor or many other ceramics. The rigidity therefore suffers accordingly.

Helium premeation is also a concern with Nylon, but helium will permeate through most nonmetals. Since the exterior of any of the ceramic or plastic concepts should be coated with a thin metallic layer, the helium permeation cannot really be considered more of a problem with any particular plastic or ceramic material. The Nylon configurations were downgraded relatively because of the rigidity problems.

The main concern with ceramics such as Macor is the residual iron content caused by iron in the raw materials. This will likely need to be reduced by special selection of the Macor or substitute ceramic. Nevertheless, Macor combines low input power, high rigidity, relatively low helium permeability and small size. These qualities make Macor the prime candidate as a material.

Vibration and Magnetic Signature

A vibration and magnetic signature analysis was performed for configurations 7, 8 and 9 because of their potential as candidate configurations. The vibration frequencies of the cantilevered cylinder/displacer assembly, each radiation shield, and the vacuum shell were determined. Table 4 gives the results of the frequency analysis for the fundamental frequency f_1, and the next 4 harmonics, f_2 thru f_5. The operating speed of the cooler is shown for comparison. In all three cases, the fundamental frequency is at least a factor of 6 higher than the operating speed. Some damping will be provided by the superinsulation in the vacuum spaces. In addition, the technique for suspending the refrigerator should be soft and should have a high damping coefficient to reduce the vibration.

An analysis of the magnetic signature noise sources and magnitude estimates has been provided by Arthur D. Little, Inc. The report of their analysis is given in the following text.

The results of this preliminary evaluation are given in Table 5. In some cases, it was possible to calculate the magnitude and frequency of the expected noise; in others, only the relative magnitudes for the designs could be assessed; and in a few cases, only a preference rating could be obtained. Where no substantial difference is expected between the designs, N.D. (no difference) appears in the Table.

TABLE 4

VIBRATION CHARACTERISTICS

Configuration	Components	lowest 5 natural frequencies, cycles/sec f_1	f_2	f_3	f_4	f_5	operating freq. cps
Small Macor	displacer cylinders	200	1260	3460	6760	11200	33.3
	outer rad. shield	670	4300	11800	23000	38200	
	inner rad. shield	1050	6700	18400	36000	60000	
	vacuum shell	630	4000	11100	21600	35800	
Macor	displacer/ cylinders	19	120	340	660	1100	1.7
	outer rad. shield	20	130	350	690	1140	
	inner rad. shield	31	200	540	1060	1750	
	vacuum shell	16	100	270	530	880	
Nylon	displacer/ cylinders	8	50	135	265	440	1.0
	outer rad. shield	55	350	960	1880	3100	
	inner rad. shield	95	610	1670	3270	5400	
	vacuum shell	40	250	700	1370	2260	

TABLE 5

RESULTS OF MAGNETIC SIGNATURE ANALYSIS

	Large MACOR	Small MACOR	Nylon
1. Ambient Noise	N.D.	N.D.	N.D.
2. Motor Noise	Low	High	Moderate
3 Displacer Field-distortion			
i. Geometric effect	1	2.82	0.65
ii. Field amplitude (gauss)	10^{-8}*	$2(10)^{-8}$*	10^{-8}
iii. Frequency (Hz)	1.7	33.3	1.0
4. Shield eddy currents	negligible	negligible	negligible
5. Charge accumulation noise			
i. Reciprocation noise (gauss)	8×10^{-14}	1×10^{-9}	4×10^{-13}
ii. Frequency (Hz)	1.7	33.3	1.0
iii. Vibration noise (gauss)	3×10^{-12}	3×10^{-9}	5×10^{-12}
iv. Frequency (Hz)	19	200	7.5
6 SQUID Vibration	Moderate	Low	High
7. Johnson Noise	N.D.	N.D.	N.D.

N.D.; No Difference

* Note:

These figures were calculated using the Weiss theory of ferromagnetism, assuming that the iron atoms (with a number of order 10^{19}/cc (i.e. 500 PPM)) are uniformly distributed and isolated from each other in Macor. If this assumption is correct, the calculated Curie temperature is about 0.2K, so that, at the operating temperature, paramagnetic behavior is expected. If the impurity instead consists of isolated aggregates of iron atoms, each comparable to or larger than a domain in size (that is about 10^{15} atoms), the material will behave like a collection of small ferromagnets and much higher susceptibility would be obtained. This question can be resolved only by an experimental investigation which is recommended before using a Macor displacer in a cryocooler for this application.

The potential noise sources include:

- Ambient noise due to aircraft systems, geomagnetic noise, etc. This noise is expected to be comparable in all three refrigerator designs. Design of the overall magnetometer systems for best performance in the presence of this noise is a separate subject, not considered here.

- Noise due to electrical components of the refrigerator, such as the motor driving the displacer. Other factors being equal (similar refrigerating capacity and efficiency, similar motor designs), the largest concept (Large MACOR) would be preferred because the motor is farthest away from the SQUID. Careful attention should be given to magnetic shielding of the motor. In order to minimize noise in the signal frequency range, a 400 Hz geared motor is preferable to a DC motor. If necessary, the refrigerator could be driven by compressed air, allowing remote location of the electrical drive.

- Distortion of the terrestrial field by the displacer. For the simplest case, in which the terrestrial field is aligned with the axis of the displacer, the variation in the field on axis at a distance Z_o from the mean position of the end of the displacer piston is given approximately by

$$H = 1/2 H_o \chi \frac{a^2 \delta}{(Z_o^2 + a^2)^{3/2}} \qquad (17)$$

where δ is the stroke of the displacer, a is the radius of the displacer in the final stage, χ is the magnetic susceptibility of the displacer material, and H_o is the terrestrial field. The fundamental frequency of this noise is of course that of the displacer.

The value of $a^2\delta/(Z_o^2+a^2)^{3/2}$ is shown in the Table as ("Geometric Effect"), normalized to that for the large MACOR design. This shows what the relative magnitude of this noise would be if all designs used the same material for the displacer. It is clear that changes in the dimensions can have a significant effect on this noise.

The volume susceptibility of nylon at 10K varies from about 10^{-5} (Gaussian Units) down to zero or perhaps to diamagnetic values [12]. The upper bound on the amplitude of the field-distortion noise for the nylon-displacer design is calculated as 10^{-8} gauss, but it could be significantly smaller if nylon selected for near-zero susceptibility were used.

The upper limit specification for Macor is 1000 PPM of iron, although typical samples are expected to contain about 500 PPM [13]. Experiments at 4K in the terrestrial field gave a MACOR susceptibility which was too low to measure [13]. We suspect that the sample used in this experiment had little or no ferromagnetic contamination. It is clear that great care must be taken to avoid introduction of ferromagnetic particles, for example, during machining of the displacer. Special manufacturing methods may be needed to reduce the residual iron content caused by iron in the raw materials [13]. The field amplitudes reported for the Macor concepts in Table 5 were calculated using 500 PPM of iron.

- Eddy currents. Vibrations of the radiation shields within the earth's field will induce currents in them. However, rough calculations indicate that the field fluctuations at the SQUID due to these effects will be of order 10^{-15} gauss or less, below the inherent noise level of the device. The use of superinsulation will in any case tend to damp these vibrations.

- Electrostatic charge. Charge build-up on the displacer piston will produce electric fields in the vicinity of the SQUID, and motion of the displacer will then induce magnetic fields. Reciprocating motion of the displacer will create circumferential magnetic fields about the axis, with zero field on the axis. Vibration of the displacer will create fields perpendicular to the vibration.

  In order to estimate an upper bound to the magnitude of these effects, we arbitrarily assumed that electrostatic charging could elevate the potential of the end of the displacer by up to 1000 volts above that of the cylinder end. The field due to reciprocating motion was then calculated at a point 1 mm off axis at the location of the SQUID, with the

results given in the table. For the vibration-induced field, we arbitrarily assumed that the amplitude of the vibration of the displacer end was 10% of the clearance between it and the cylinder wall, and the field was calculated on axis at the SQUID location.

Because of the dubious assumptions in this calculation, the fields given should be considered accurate only to within an order to magnitude or more, but they are probably high. In any case, the SQUID could be protected from this noise by plating the outside of the displacer cylinder with a thin metal coating, and this is recommended.

- SQUID vibrations. The SQUID is mounted on the end of a beam whose vibrations will change its orientation with respect to the terrestrial field. If the angular amplitude of vibration is α, the magnetic noise from this effect is simply $H_0\alpha$. The refrigerator suspension should be designed to be soft with a lot of damping at the beam vibration frequency. Care is clearly needed to make this effect small. Other factors being equal, the design with the highest beam vibration frequency is preferred with respect to this effect, so as to remove this noise source as far as possible from the signal band.

- Johnson noise. Thermal noise currents are expected in the radiation shields and superinsulation, and these will produce magnetic noise at the SQUID. Since the amplitude of Johnson noise varies inversely with the frequency, this noise source could be significant in the signal band. Explicit calculation of the noise requires more information than is presently available (e.g., the temperature distribution in the shields). Such a calculation might suggest ways to reduce Johnson noise. With respect to Johnson noise fields, the present radiation shields act like long solenoids, so that the fields at the SQUID depend on the shield temperatures but not on their dimensions. The three designs are thus expected to be comparable in their sensitivities to this effect.

Recommendations From Magnetic Analysis

- A well-shielded AC motor should be used to drive the refrigerator. A compressed-air drive would be preferable.

- Great care should be taken to avoid ferromagnetic contamination of the displacer and cylinder during machining.

- The susceptibility of Macor should be made as small as possible by the manufacturing process and by elimination of iron contamination during machining. Nylon susceptibility should be chosen as near zero as possible by choosing the proper nylon material.

- The outside of the displacer cylinder should be plated to minimize moving charge effects.

- Careful attention should be paid to damping beam vibration modes affecting the SQUID mounting and to avoid excitation of these modes.

- The lead slug for thermal smoothing is acceptable only for working temperatures above the superconducting transition temperature of lead. A lead damping block is therefore not acceptable for 4.2K operation.

- An analysis should be undertaken of Johnson magnetic noise and of means for minimizing this effect.

- Design of the refrigerator should be integrated with overall design of the magnetometer. For example, an external Helmholtz coil to buck out the terrestrial field would minimize displacer field-distortion noise. Some of the noises may be filtered by signal processing, and others might be reduced by magnetic feedback using small coils near the SQUID.

V. CRITICAL AREAS

Concepts presented in this report have some critical areas that need additional attention. These are identified in the following text and approaches to solutions are suggested.

Plastic and Ceramic Materials:

- Helium can permeate by diffusion through the plastic and glass materials proposed in the gap concepts.
- Electrically non conductive materials used to construct the displacer and cylinder walls can develop static electrical changes. Motion of these charges through the Earth's field can produce a magnetic signature at the electronics.

Metals

- Metals act as magnetic signature sources due to the generally higher magnetic susceptibility and because of motion of the electrical conductor through the Earth's magnetic field.

Vibration:

- Reduction of vibration to the required levels is challenging. Special attention needs to be addressed to the method of mounting the cryocooler to provide additional damping and support to the cold finger, radiation shields and vacuum shell, and to methods of isolating the electronics from the cold finger.

Drive Motor Magnetic Field:

- Careful attention will be needed for proper shielding to attenuate the motor magnetic field.

Approaches to Critical Areas

Plastic and Ceramic Materials:

Helium can diffuse through almost any ceramic or plastic material. These materials will therefore need to be coated with a layer impervious to helium. This layer will very likely need to be a metal. While helium can also diffuse through some metals, the rate is generally much lower. The metallic coating necessary for an impervious layer is generally very thin. This thickness needs to be a trade off between achieving an impermeable layer and minimizing the axial thermal conduction loss in the cryocooler. Thicknessess less than 0.002 centimeters are generally acceptable for conduction losses. This is more than enough to produce an impermeable coating. Approaches for achieving the impervious coating are:

- Impregnating the plastic material with a penetrant that seals the helium diffusion paths.

- Coating the outside of the plastic cylinder with an impermeable coating.

In the first approach, the cylinders are treated before assembly. They are placed in a chamber which is then evacuated. Next a sealant, preferably a metallic sealant, is admitted and the cylinders are immersed while in a vacuum. High pressure air is then admitted to the chamber to finish driving the sealant into the diffusion paths of the material. Manufacturers have claimed that the process will seal extremely minute porosity; however, conversation with a manufacturer indicate that the process has not been used to seal the small interstities in plastics. The sealant itself must be impervious to helium; therefore, the metallic sealants that are para- or dia- magnetic are preferable.

The process has been used to seal metallic castings. Testing of the effectiveness of sealing ceramics and plastics will need to be done. Particular sealants by various manufacturers will need to be tested to determine the one that is most effective. Many sealants that appear to seal castings completely may still be permeable to helium. The same sealant may not penetrate into the very small interstructural diffusion paths in ceramics and plastics.

The second method includes coating the cylinder with metallic coatings or possibly with impermeable epoxy or similar materials. A metal with very low magnetic susceptibilty such as gold, copper or possibly indium can be coated onto the cylinder by the sputtering process. The thickness can be adjusted so as to give an impermeable barrier to helium but present a low axial heat conduction loss. Calculations indicate that metal thicknesses less than approximately 1 mil will produce an acceptably low conduction loss. This is considered a very thick coating with regard to making an impermeable barrier.

A coating of epoxy or other material onto the outside of the cylinder can be an alternate method of making an impermeable layer on the exterior of the cold finger Epoxy, parylene, and similar coatings have had mixed success in sealing against helium. More investigation to establish the validity of a nonmetallic coating is needed.

The approach to the static electricity generation is to plate the outside of the cylinder assembly with a metal such as indium. This solution can be combined with the metal coating approach to the helium permeation problem since the coating will likely solve both problems. The metal coating approach is therefore recommended.

Metals

Metals moving in magnetic fields cause electric current generation. Local magnetic field perturbations are therefore produced. The use of metals, particularly metals with appreciable movement, should be avoided. Cryocooler displacers and moving components near the cold end should be made of non metals. Even metal vibration will be disruptive. In the present program, the damping block is constructed of lead because of its thermal properties. The metallic coating to solve the static and permeation problems may result in magnetic signature because of a vibrating metal located near the cold end. Care must be taken, therefore, to minimize the vibration. Only absolutely necessary metal construction should be used.

Vibration

Vibration is probably the most critical of the areas of concern. Reduction of vibration so that the electronics moves through an angle of 10^{-10} radians or less is very difficult. While the concepts included in this report are attractive because they use a minimum of metallic construction and a minimum of power, isolation of the electronics from the cryocooler may very likely be needed to achieve the program vibration goals. The integral drive system will have less vibration than a split system because a greater degree of balancing can be achieved; however, isolation of the electronics may be the only way to achieve the vibration goals. Possible isolation methods include a flexible conduction link, and a wire mesh thermal contact. A radiation link has been used at higher temperatures (77K), but the low temperatures involved will preclude this method. It should also be noted that conduction lines are not infinitely flexible. They also carry some vibration. Nor is vibration limited to the type of cycle selected for these concepts. The use of a Claude type cycle also has inherent vibration noise. A Joule Thomson expansion used in Claude cycles introduces the vibration noise of gas expanding through the J-T valve. The spectral definition of that noise is not well defined so that electronic methods of reducing noise are more difficult.

The gap concepts addressed in this report appear to be attractive for applying electronic suppression of vibratory noise interference. The displacer and compressor frequencies of operation are well defined. The beam vibration frequencies can also be predicted reasonably well so electronic counter measures can be designed. A Helmholtz coil bucking system can be of value in reducing the displacer field distortion noise. Beam vibration noise will probably yield to a similar treatment. In general, filtering during the signal processing and electronic noise suppression are reasonable approaches for reducing the effects of vibration.

Drive Motor Magnetic Field

Mu metal shielding must be used to reduce the motor magnetic field. Several layers of Mu metal will probably be needed to achieve the required attenuation.

VI. THERMODYNAMIC PERFORMANCE

The configurations listed in Table 2 are designed to produce 50 milliwatts of refrigeration at 10K. Appropriate safety factors have been used in relating the mathematical model predictions to expected performance. The performance of the configurations used for concepts in columns 7, 8, 9 at 8.5K were estimated using the model even though some of the data correlations have a lower limit of 10K. The 8.5 K performance was combined with the 10 K performance to extrapolate to the zero load temperature. Therefore, the 8.5 K and zero load temperatures must be considered as estimates only. The 10K and 8.5K, capacities and zero load temperatures for the small Macor, Macor, and Nylon configurations are given in Table 6. The small Macor and Nylon configurations have about half of their 10K capacity left at 8.5K whereas the larger Macor configuration will have zero capacity at about 8.5K. Larger thermal losses are associated with the larger Macor configuration. The losses produce the steeper net change of capacity with temperature.

The trend of required input power as a function of the number of stages for the Macor configurations is shown in Figure 6. The input power requirements for the small and larger four stage configurations are shown to indicate that there is a spread in representing this trend. There is an effect of size and other system parameters on the input power of four stage configurations or configurations representing any given number of stages. The trend is, therefore, only approximate, but it does show a decreasing power requirement as the number of stages is increased. However, the addition of stages has diminishing returns. The input power reduction to be gained by the use of five stages instead of four is less than the reduction to be gained by the use of four stages instead of three. The trend of Figure 6 shows that the slope of the input power with number of stages is fairly flat at five stages, i.e., four stages are almost as attractive as five. Since more stages can be equated to greater complexity, a judgement must be made in the selection of stages. Four stages were therefore chosen for the concepts. The model indicates that three or even two stages could have been used, albeit with a greater power requirement. The choice of four stages was a compromise between input power and complexity.

TABLE 6

GAP CONCEPT PERFORMANCE

CAPACITY AT TEMPERATURE, (mW)

Configuration	10K	8.5K	Zero Load Temperature, K
Small Macor	50	30	6.5
Macor	50	0	8.5 to 9.0
Nylon	50	21	7.5

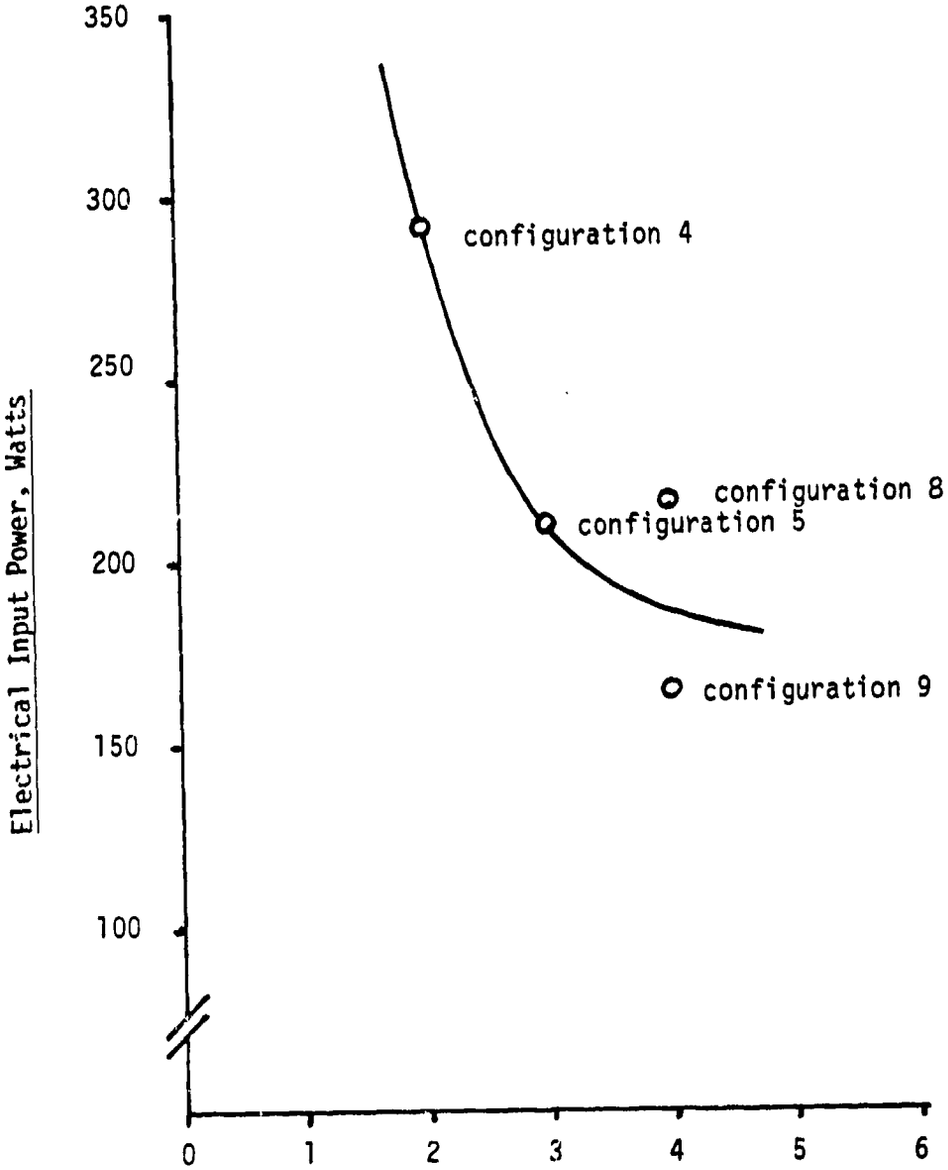

Figure 6: Macor Configurations
Trend of Input Power
Vs. Number Of Stages

Gap configurations are very dependent on the thermal penetration required to serve as an effective regenerator. One representation of the thermal penetration depth is given by λ, the depth required for the cyclic temperature amplitude to decay to 1/e of its value at the regenerator surface. In order to have an effective regenerator, the cylinder wall thickness (and the regenerator annular wall in the displacer) must be a multiple, (e.g., at least four times), of the λvalue. Structural considerations may dictate even thicker walls.

The λ thickness as a function of operating temperature is shown in Figure 7 for the small Macor configuration. The λ is the reciprocal of the logarithmic decrement, equation (10). Since the specific heat decreases faster with temperature than the thermal conductivity, λ increases with decreasing temperature as shown for Macor in Figure 7. The cylinder walls of the colder stages are thicker to account for the larger penetration depths. The conduction loss in the colder stages which have thicker walls is offset by the lower thermal conductivity at the lower temperatures.

The λ is also a function of the operational frequency as shown in Figure 8. Since λ is the reciprocal of m (equation 10), λ is a function of the reciprocal of the square root of frequency for a given temperature. A higher operating speed therefore has the advantage that thinner walls can be used to accomodate the required thermal penetration. Higher speeds have diminishing returns for Macor in this respect above 2000 RPM as shown by the relatively small slope of Figure 8 above 2000 RPM.

The trend of input power as a function of operating speed as developed using the small and larger Macor configurations is shown in Figure 9. Since only 2 points are shown, the shape of the curve is not clearly defined. The full data spread of Figure 9 is represented as prediction inaccuracy in Figure 6 for four stages. What Figure 9 does show is that the input power is at most a very weak function of operating speed between 100 and 2000 RPM. For practical purposes, input power is nearly independent of operational speed. The additional power required to cycle the system mass more often is compensated by the decreased size of the system (decreased mass flow) for concepts of the same material.

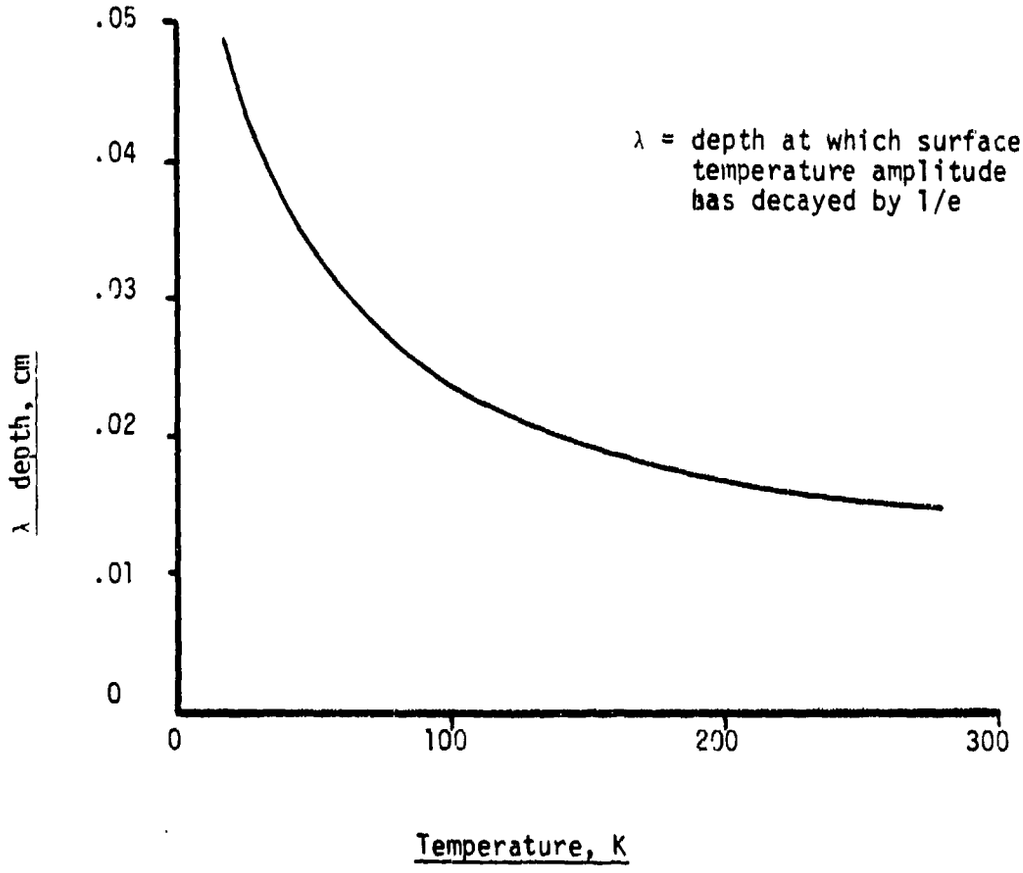

Figure 7: Macor, Thermal Depth, λ vs. Temperature

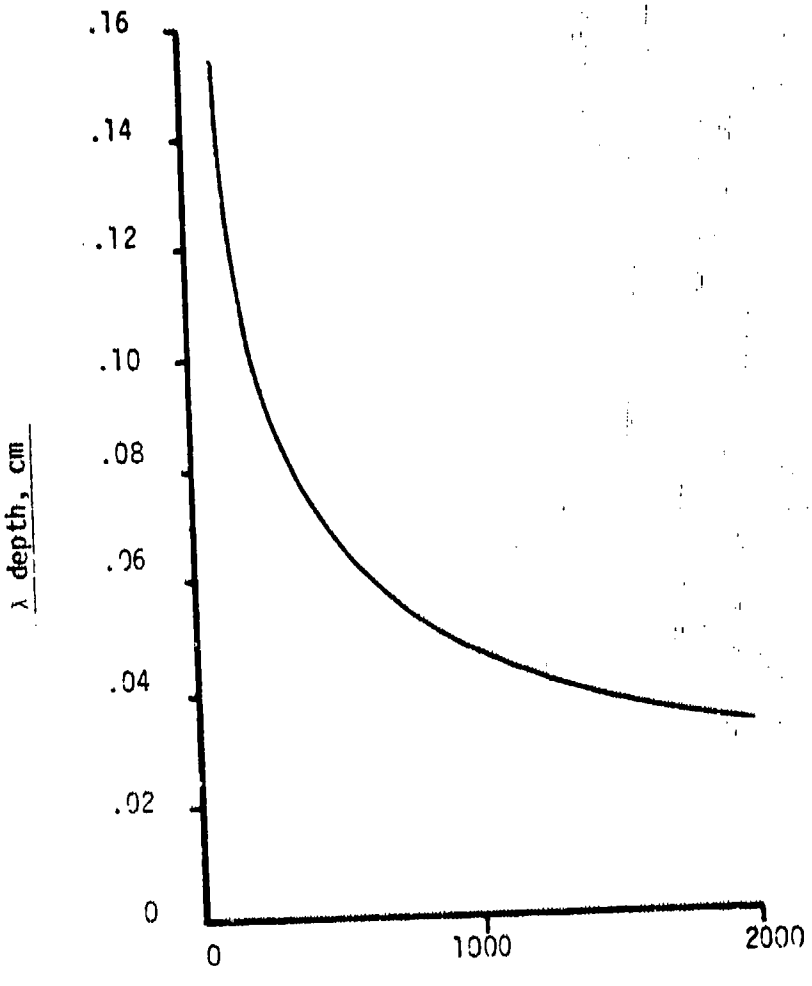

Figure 8: Small Macor Configuration,
Thermal Depth, λ,
Vs. Frequency of Operation
(Temperature = 10K)

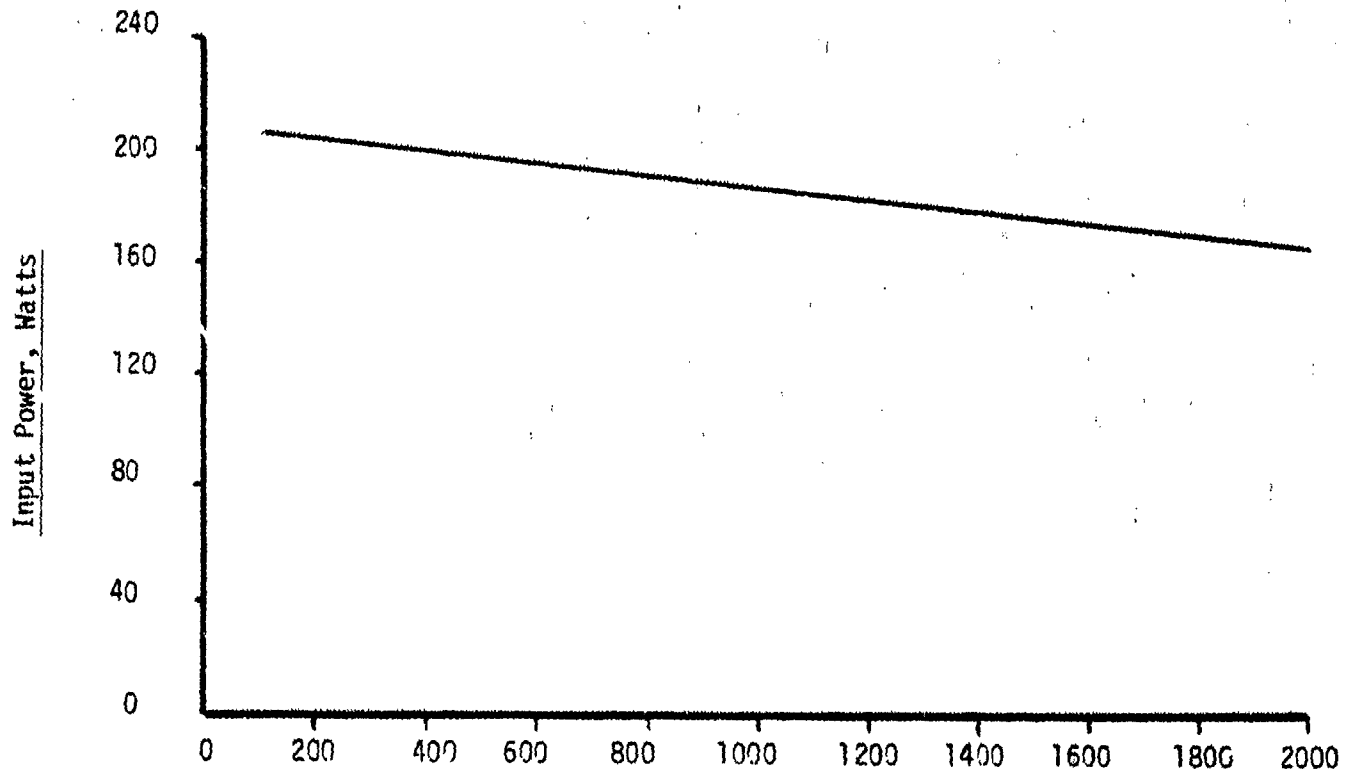

Figure 9, 4 Stage Macor Configurations
Trend of Input Power
Vs. Speed of Operation

VII. RECOMMENDED CONCEPT

Based on the results found during the course of this study, the small four stage Macor integral configuration is selected as the most attractive concept for Phase II development. Of all the configurations reported, only the large nylon has a lower power requirement. The input power required for the small Macor is 166 watts which is within the program design goal. The refrigeration capacities of the various stages of the concepts do vary somewhat because of the procedure of developing concepts for 50 milliwatts at 10K, so some power variation is expected. The small Macor first and second stages have ample refrigeration capacity to operate the radiation shields attached to them. The larger concepts need somewhat greater upper stage power, as shown in Table 2, because the radiation shields are physically larger.

The four stage small Macor configuration is the smallest of all the concepts. The relatively high operating speed is the feature that affords the potential to reduce the physical size of the design.

Ceramic materials can contain some residual iron from a small amount of iron content of the raw materials; however, the Macor material used must be a non ferromagnetic material in order to minimize magnetic interference. Special processes can be used to reduce the residual iron content if needed. All of the configurations, except the one using stainless cylinders as a comparison, are constructed of non ferromagnetic materials. The ceramic material was selected over the nylon or other plastics because it has better wear characteristics and it has superior structural rigidity.

An integral drive system is recommended with the Small Macor concept for the Phase II development. The integral drive can be more exactly balanced. Optimum balancing will result in a minimum of vibration and magnetic signature caused by vibration. The integral drive will require less power because the line loss between the compressor and cold finger is less than for a split system. A more consistent thermodynamic performance is also expected with the integral drive. The integral motor must be shielded by Mu metal, possibly by several layers, to attenuate the motor magnetic field.

The small four stage Macor integral concept is the best candidate for Phase II. This concept exhibits the greatest potential to achieve the program goals of minimum power, size, and magnetic signature.

VIII. CONCLUSIONS

The study conducted in Phase I has yielded several conclusions. They are listed in the following tabulation:

- Achievement of the required refrigeration capacity within the 250 watts input power requirement of the program is feasiable.
- Achievement of the $\pm$ 0.01K temperature tolerance at the electronics package is attainable.
- Vibration reduction to the program goals appears challenging. A method of electronics isolation may be needed.
- Residual iron in the Macor will need to be minimized in the manufacturing process.
- Ceramic or plastic materials will need to be coated, probably with a metal, to render them impervious to helium.
- An integral system is most feasible because of low input power and the capability for accurate balancing.

IX. RECOMMENDATIONS

Based on the studies conducted and the conclusions reached, the following recommendations are given:

- The small Macor concept chosen as the most attractive should be further developed into a detailed design as a Phase II effort.

- Approaches to solving the helium permeation in ceramics should be investigated in Phase II.

- Phase II should include efforts for vibration abatement including means of isolating the electronics from the cryocooler and, possibly, electronic suppression of vibration noise.

- The details of the requirements of interfacing the electronics with the cryocooler, i.e., size or space requirements, method of mounting, number of lead wires and access requirements, should be assessed as part of Phase II.

- Further investigation should be made into means of reducing the Macor residual iron content.

X. PHASE II PROGRAM PLAN

The plan for the proposed Phase II development includes a definition of the objective, an overview of the scope, and a description of suggested tasks to accomplish the objective.

Objectives

The objective of Phase II is to produce a cryocooler design sufficiently detailed for complete evaluation and for construction of a prototype unit.

Overview of Scope

The scope of Phase II comprises a cryocooler interface definition, and the detailed design including a magnetic signature analysis. The definition of interface requirements includes discussions with SQUID manufacturers and with the Navy to determine mounting requirements, power requirements, and details of vibration and magnetic signature allowances. The results of the interface definition will be used in the Phase II design.

Vibration isolation is a critical area identified in Phase I. Additional study of methods of isolating the electronics from cryocooler vibration must be pursued. Separation of the electronics from the cryocooler is an area that needs additional investigation. Investigation of the method, geometry, and construction is included in the Phase II plan.

Overview of Tasks:

- The first task is a study of the interface requirements of the electronics. Discussions with SQUID manufacturers and with the Navy are to be used to establish power dissipation, space requirements, mounting details, vibration requirements, and magnetic shielding requirements of the electronics. The study will be used to define the number of lead wires, their geometry and other access requirements.

- The primary task is a detailed design of the small Macor concept. The sub tasks of the detailed design are described in the following paragraphs.

A thermodynamic analysis including performance predictions, and a cool-down time analysis is to be included. The small Macor concept will be modified as necessary based on the analysis.

The approaches for eliminating helium permeation through Macor identified in Phase I are to be pursued to produce a design which includes a method of eliminating helium permeation.

An investigation of vibration isolation is needed to identify the most attractive method of achieving vibration goals. This sub task defines the method of isolation to be used in the mechanical detailed design.

A mechanical detailed design is to be carried out including methods of assembling and fastening the cylinders, radiation shields, and various components. Design drawings are to be the result of this sub task.

An analysis of vibration and magnetic signature is to be made of the design. Results are to be used to modify the design to correct deficiencies.

- The final report will describe the detailed mechanical design, vibration and magnetic signature analysis, and the thermodynamic performance predictions. It will also include the results of the impervious coating method evaluation program, the interface definition task, and the vibration isolation task.

Program Schedule:

The proposed schedule for Phase II is shown in Figure 10. A nine month Phase II program is proposed. Reviews are to be held at the end of 3 months and 6 months from the date of contract award. Monthly progress reports are proposed. The proposed final report due date is 9 months after contract award.

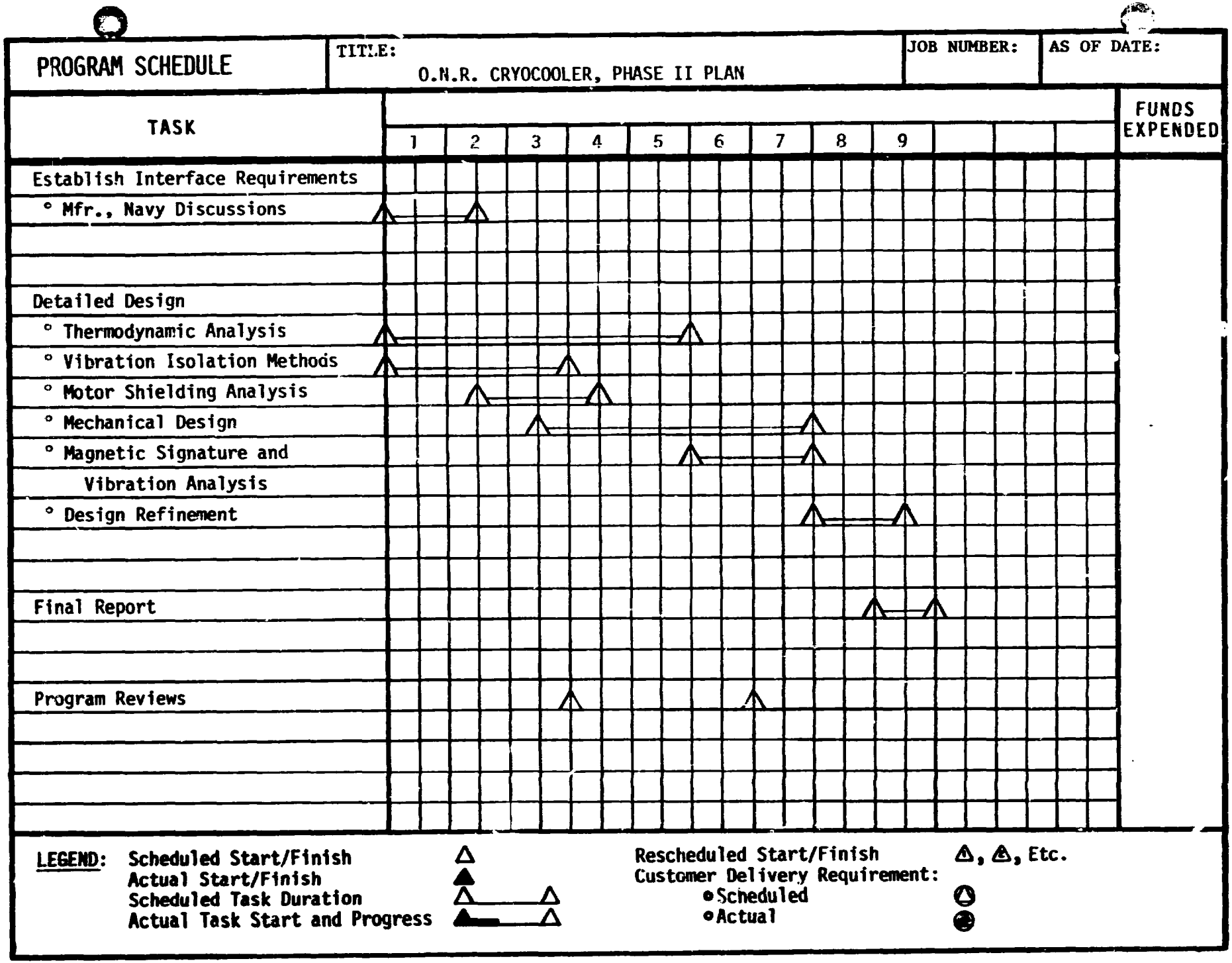

Figure 10: Phase II Program Schedule

APPENDIX

COMPARISON OF GAP MODEL PREDICTIONS WITH EXPERIMENTAL DATA

In order to calibrate the model for performance predictions of gap regenerative systems, the model predictions were compared with experimental data reported by NBS for 3 stage [11], 4 stage [14], and 5 stage [15] cryocoolers. The 3 stage, 4 stage, and 5 stage comparisons will be discussed in the following subsections. Then reasons for differences in results will be suggested and the method of using the comparison to calibrate the model predictions will be described.

Three Stage System

The three stage model described in [11] achieved a no load third stage temperature of 12.5 to 13K. With an applied load of 11 milliwatts, the temperature increased to 14.5K. The input power reported from assuming isothermal compression was about [illegible] watts at the no load condition. Comparison of the model prediction with the NBS results is shown in Table 7. The geometry and conditions used in the comparison are NBS values as reported in the literature except for high and low pressures and second stage temperature. Pressures were calculated based on the average charge pressure. The second stage temperature was estimated as 40K. The stage temperatures are inputs to the model. The resulting capacities predicted by the model are higher than the experimental capacities, but the input power requirements compare closely.

Four Stage System

The four stage refrigerator described in [14] achieved 8.5K with no applied load. The input isothermal power was about 15 watts as in the three stage system. The model prediction was 22 milliwatts at 8.5K. Table 8 gives the comparison of the model predictions with the data and also gives the geometry and conditions for the four stage system. Temperatures of the upper stages were not reported in the literature and are therefore estimated. High and low pressures were calculated from the average pressure and the volumes of the expander, compressor, and other elements of the system. Predicted capacities are also higher than experimental capacities for the four stage system. Input power requirements again compare closely.

TABLE 7

MODEL PREDICTIONS COMPARED

TO NBS RESULTS -- THREE STAGE SYSTEM

	NBS RESULTS		MODEL PREDICTION	
T_3,K	Capacity,mW	Isothermal Input Power, Watts	Capacity,mW	Isothermal Input Power, Watts
13	0	15	49	17.2
14.5	11	--	50	16.4

GEOMETRY AND CONDITIONS

	1st stage	2nd stage	3rd stage
dia., mm	19	9.5	4.7
length, mm	245	143	144
gap, mm	0.05	0.07	0.04
wall thickness, mm	2.4	2.4	2.4
temperature, K	120	40 *	13

*estimated

Nylon displacers and G10 Cylinders

Average pressure 5.0 atm.

Minimum pressure 3.0 atm. (calculated)

Maximum pressure 8.2 atm. (calculated)

TABLE 8

MODEL PREDICTIONS COMPARED

TO NBS RESULTS -- FOUR STAGE SYSTEM

	NBS RESULTS		MODEL PREDICTION	
T_4,K	Capacity,mW	Isothermal Input Power, Watts	Capacity,mW	Isothermal Input Power, Watts
8.5	0	15	22	18.47

GEOMETRY AND CONDITIONS

	1st stage	2nd stage	3rd stage	4th stage
dia., mm	28	19	9.5	4.7
length, mm	120	120	100	150
gap, mm	0.140	0.079	0.048	0.023
wall thickness, mm	4	4	4	4
temperature, K	180 *	80 *	30 *	8.5

* estimated

Nylon displacers and G10 Cylinders

Average pressure 5.0 atm.

Minimum pressure 3.1 atm. (calculated)

Maximum pressure 8.0 atm. (calculated)

Five Stage System

Comparison of model predictions and NBS data [15] was made to help to determine the model calibration. Even though a five stage concept was not included as a study result, the comparison was used as an additional check on the model. The five stage system achieved an experimental temperature of about 6.8K with no external applied load. In addition, several temperatures were measured with various external loads. The comparison of data and model predictions is given in Table 9. The geometry and conditions are also reported in the table. While the property correlations of the G10 and Nylon used in the model should be valid to about 5K, the specific heat correlation used for helium has an accuracy of 2% only down to 10K. Therefore, the comparison for the five stage system below 10K will probably have less accuracy.

Whereas the maximum and minimum pressures of the 3 and 4 stage systems had to be calculated based on the geometry and the measured average pressure, the pressure extremes of the five stage system were reported in the literature. At 9K, the difference between data and the model prediction is about 20 mW. The difference increases to about 28 mW at 6.8K possibly because the temperature is further from the lower limit of the specific heat correlation. The same comment can help to explain the difference of 38 watts between the predicted and reported input power values. Since this is only one of the three comparisons and it is outside the range of the model specific heat correlation, the importance of this input power comparison should be minimized.

A review of the model predictions indicates a difference between data and prediction at temperature of about 30 mW for the three stage system, 22 mW for the four stage, and about 28 mW for the five stage system. The model overpredicts capacity in each case by these amounts. It is possible that the experimental apparatus had extraneous heat leaks that reduced the net or apparent capacity. In this case, a model would not include apparatus losses that are not part of the thermodynamic losses discussed in the description of the model. One way to handle the difference is to say that the model should be calibrated to include the extra losses. The overpredictions were therefore subtracted from the concept 10K performance. In addition, a safety factor of 2 was used for the 10K performance of the concepts.

TABLE 9

MODEL PREDICTIONS COMPARED

TO NBS RESULTS -- FIVE STAGE SYSTEM

	NBS RESULTS		MODEL PREDICTION	
T,K	Capacity,mW	Isothermal Input Power, Watts	Capacity,mW	Isothermal Input Power, Watts
6.8	0	--	28.5	--
7	1.5	20	29	57.9
9	12.5	--	32	53.9

GEOMETRY AND CONDITIONS

	1st stage	2nd stage	3rd stage	4th stage	5th stage
Dia., mm	38	29	19	9.5	4.8
Length, mm	140	130	120	83	133
Gap, mm	0.23	0.23	0.18	0.10	0.05
Wall thickness, mm	3.2	2.4	2.4	2.4	2.4
Temperature, K	167	70	27	15.5	7

Nylon displacers and G10 Cylinders

Average pressure 3.0 atm.

Minimum pressure 1.6 atm.

Maximum pressure 5.7 atm.

The model overpredicts isothermal power by 2 W for the three stage cooler, 3.5 W for the four stage cooler, and 40 W for the five stage system. The power overprediction increases as the temperature drops further below 10K for the five stage system. Therefore, the correlation limit problem may be effecting the power calculation. These experimental data were the only ones readily available so far as we know. We used them for comparison even though some points were outside the ranges of the property correlations. It is difficult to say whether the experimental data had inaccuracies or whether the predictions are inaccurate. It can just be said that the discrepancies are present. In each case, the model power requirement is higher than the experimentally measured power. The power requirements given by the model appear, therefore, to be conservative, i.e. a system designed with the model won't require more power than the model indicates.

REFERENCES

1. Andeen, B.A., Performance Modeling, CTI-CRYOGENICS Internal Report (1978)

2. McAdams, W.H., Heat Transmisssion, McGraw Hill (1952)

3. Kays, W.M., and London, A.L., Compact Heat Exchangers, McGraw Hill (1964)

4. Corruccini, R.J., and Gniewek, J.J., Specific Heats and Enthalpies of Technical Solids at Low Temperature, Wright Air Development Center, Published by N.B.S., Boulder, Colorado (1960).

5. Touloukian, Y.S., Powell, R.W., Ho, C.Y., Klemius, P.G., Thermophysical Properties of Matter, The TPRC Data Series, IFI/Plenum (1970)

6. Johnson, V.J. (Editor) "A Compendium of the Properties of Materials at Low Temperature" WADD Technical Report 60-56, Parts I and II, Wright Air Development Division, U.S. Air Force, Wright Patterson Air Force Base, Ohio (1960)

7. Radebaugh, R., National Bureau of Standards, Boulder, Colo., Private Communication

8. Jakob, M., Heat Tranfser, Vol 1, John Wiley and Sons, (1962)

9. Radebaugh, R., Analysis of Inefficiency of Gap Type Regenerators", Proceedings of 15th International Congress of Refrigeration, Venice (1979)

10. Norris, R.E. (Editor), Heat Transfer Data Book, General Electric Co., Schenectady N.Y. (1977)

11. Zimmerman, J.E., Radebaugh, R., and Siegwarth, J.D., "Possible Cryocoolers for SQUID Magnetometers", Proceedings of the International Conference on Superconducting Devices, Berlin (1976)

12. White, G.K., Experimental Techniques in Low Temperature Physics, P.203, Clarendon Press, Oxford (1968)

13. Wahl, J., Corning Glass Company, Private Communication.

14. Zimmerman, J.E., and Radebaugh, R., "Operation of a SQUID in a Very Low Power Cryocooler," NBS Special Publication 508, P.59 (1977)

15. Zimmerman, J.E., "Cryogenics for SQUIDS", Electromagnetic Technology Division, National Bureau of Standards, Boulder, Colorado (Obtained by private communication (1980))